3.2. Case 2

A 49-year-old woman, a non-smoker with no history of illness, PS0, was introduced to the Orthopedics Department of our Center in April 2009 for back pain and multiple osteoplastic changes in the bones. Systematic examination revealed an abnormal shadow 22X13 mm in size in the left lower lobe (Fig. 4A). Bronchoscopy and a PET scan indicated left S8 adenocarcinoma with cervical, axial, mediastinal, hilar, pancreatic and retroperitoneal lymph node metastases, as well as cranial, thoracic (Th1-12), lumbar (L1-5), rib (1–12) pelvis, humerus, and femur metastases (Fig. 5A).

She refused any therapy except for best supportive care. One month after the examination, an additional immunohistochemical examination for EML4-ALK fusion protein was performed, and found to be positive. The presence of mRNA for EML4-ALK gene was also confirmed by RT-PCR and FISH from the mediastinal #4R lymph nodes obtained with EBUS-TBNA, which was performed 2 months later. EGFR mutation was negative, but the direct sequence of the EML4-ALK mRNA indicated that the translocation was variant 3 [9]. She decided to be enrolled to the crizotinib study (PF02341066) at a dosage of 500 mg/day at Seoul National University from July 2009.

She had nausea, diarrhea and light image persistence as in case 1, but her gastrointestinal symptoms were severer than those in case 1. Two weeks after the administration of ALK inhibitor, her back pain disappeared. A PET scan performed 5 weeks after the initiation of the therapy showed marked reduction of bone and lymph node metastases, and the primary tumor had decreased in size from 22X13 mm to 12X7 mm (Fig. 4A and B). Also, the SUV max dropped from 10.7 to 2.42. Changes of tumor markers were not parallel with the clinical course since the measured value of CA-125 dropped from 424 to 107 U/ml, but that of CEA increased from 21.5 to 65.4 ng/ml 4 months later. The value of CEA then gradually decreased to 15.2 ng/ml in April 2010 (10 months after that: Fig. 6). The PET scan conducted after 7 months indicated a partial response to multiple bone and lymph node metastases (Fig. 5B). The patient continued to take the drug until the end of July 2010, when brain metastases (Fig. 7) were found.

3.3. Case 3

A fifty-four-year-old woman, also a non-smoker, PS0, visited a doctor because of back pain in August 2008. Chest X-ray and CT scan showed an S3 59X22 mm tumor in the right upper lobe, combined with #4R, #2R mediastinal lymph nodes and intrapulmonary metastases. The tumor had invaded the SVC and the azygos vein. She had undergone bronchoscopy and EBUS-TBNA in October 2008. A diagnosis of lung adenocarcinoma was obtained with TBNA samples from #7 lymph nodes. Bone scans indicated cranial, costal, vertebral, scapular, pelvic and femoral metastases (T4N2M1 stage IV). She received 2 courses of CBDCA + GEM (1000 mg/m^2) and 7 courses of docetaxel (TXTL: 60 mg/m^2) from November 2008 to June 2009, but the effect was minimal.

EML4-ALK fusion gene was suggested immunohistochemically in August 2009 and confirmed by RT-PCR obtained by EBUS-TBNA samples from the primary tumor in September 2009. She was enrolled for the clinical trial from November 2009 with an oral administration of crizotinib 500 mg/day. Dyspnea and cough were alleviated within 2 weeks, and she complained of severe diarrhea, nausea, vomiting, light image persistence and perceived changes of taste. A PET scan one month after the start of the treatment demonstrated complete disappearance of the primary tumor as well as all the metastases except for a bone metastasis to the right 8th rib. A PET scan follow-up 8 months later indicated complete control of primary and metastatic tumors (Fig. 8A and B). CEA declined slowly from 1764 ng/ml to 79 ng/ml 6 months after the start of administration (Fig. 9). The patient had 12 brain metastases from 5 mm^3 to 309 mm^3 in volume and underwent gamma knife irradiation in August 2009, 2 months before the start of ALK inhibitor treatment. The irradiated field still showed little change for 5 months, but small new lesions appeared in the left occipital area 6 months after the start of the trial. Brain metastases grew very slowly, so we have maintained our observation until October 2010.

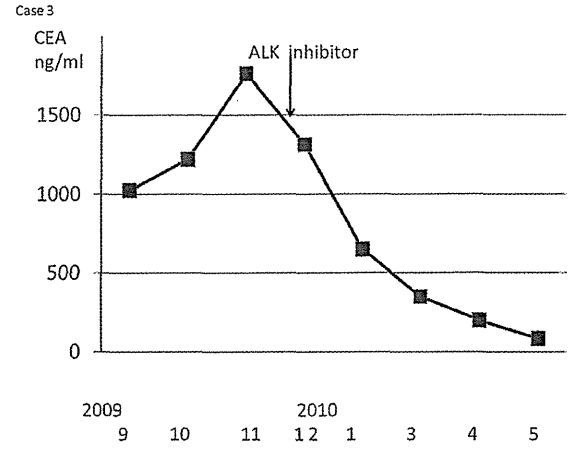

Fig. 9. CEA (■) declined slowly from 1764 ng/ml to 79 ng/ml 6 months after the start of the therapy in case 3.

4. Discussion

Above, we have reported the far-reaching effects of an ALK inhibitor on *EML4-ALK*-positive lung cancer patients. Soon after the administration of crizotinib, almost all metastases to bone and lymph nodes rapidly disappeared, followed by a marked reduction in the level of tumor markers in the sera. These observations clearly support the pivotal role of EML4-ALK oncokinase for the growth/survival of not only primary tumors but of the metastases. Such profound effects were rare among the patients when treated with conventional cytotoxic anticancer drugs.

The three cases which were enrolled for the study had surprisingly similar biological characteristics. They had multiple bone and lymph node metastases at the first medical examination, and were non-smokers at younger ages (48–54) who were resistant to chemotherapy. Adverse effects with crizotinib were also similar among them, including transient diarrhea, nausea, light image persistence, and subjective changes of taste. In addition, their response to ALK inhibitor was similar. Bone and lymph node metastases had disappeared within one month after the initiation of the therapy. The response of the primary tumor in case 2 was relatively slow compared with those of the metastases. The difference between the response of primary tumor and metastases to the ALK inhibitor in this case seems to indicate that the similar subclones of tumor cells in the primary tumors that were highly responsive to ALK inhibitor metastasized to distant organs and may give some explanation for the discrepancy in the time-course between CEA and CA125.

Molecular and immunohistochemical analyses in this cohort were conducted on the basis of the specimens obtained through EBUS-TBNA. Originally, EBUS-TBNA had been proposed useful for the pathological diagnosis of mediastinal involvement (N2 disease) of lung cancer [17–20]. However, we have already reported that EBUS-TBNA is also a versatile way of obtaining histological samples for the molecular analyses of cancer-related genes, such as *EGFR*, p53 et al. [21,22]. For those who have advanced NSCLC, it is often difficult to conduct surgery to obtain specimens from patients. Among such cases, however, EBUS-TBNA can usually be safely carried out to obtain specimens from enlarged mediastinal

lymph nodes or parathracheal tumors. We carried out EBUS-TBNA procedure for the reasons of its advantage in obtaining high quality core samples adequate for this purpose as well as its safety. We do not disregard the importance of TBB for the diagnosis of lung cancer; however, we needed histological samples to examine the immunohistochemistry and FISH for enrolment in a trial of crizotinib. Our experience with the three cases clearly demonstrates the importance and clinical relevance of obtaining such specimens for molecular analyses.

Although the initial effects of crizotinib are substantial in our cases, as well as in those reported by Bang et al. [10,11], such efficacy may not always last long. There was, for instance, development (case 1 and 2) and recurrence (case 3) of brain metastases while favorable control was maintained outside the brain. Given that the primary tumors and lymph node metastases were under control of crizotinib even at the appearance of brain metastases, the tumor cells outside the brain did not lose sensitivity to crizotinib. Relapses in the brain only may indicate either (i) subclones of the tumor acquired both the homing ability to the brain and resistance to crizotinib, or (ii) crizotinib may not penetrate the blood-brain barrier, leading to insufficient concentrations of crizotinib in the brain. It is thus highly important to examine in detail the molecular basis that would account for such acquired resistance to crizotinib, which may be secondary mutations within EML4-ALK itself or mutations/gene amplification of other genes, as demonstrated in the cases of acquired resistance of NSCLC to gefitinib/erlotinib [23–26].

Conflict of interest

None declared.

Acknowledgements

We are grateful to Dr. Yung-Jue Bang and the medical staff of Seoul National University Hospital for their support in the treatment of these patients. We also thank Mr. C.W.P. Reynolds of the Department of International Medical Communications, Tokyo Medical University, for his careful revision of the English of this manuscript.

References

[1] Janku F, Stewart DJ, Kurzrock R. Targeted therapy in non-small-cell lung cancer—Is it becoming a reality? Nat Rev Clin Oncol 2010 Jun 15;7(July (7)):401–14.
[2] Heinrich MC, Owzar K, Corless CL, et al. Correlation of kinase genotype and clinical outcome in the North American intergroup phase III trial of imatinib mesylate for treatment of advanced gastrointestinal stromal tumor: CALGB 150105 study by cancer and leukemia group B and southwest oncology group. J Clin Oncol 2008;26:5360–7.
[3] Mok TS, Wu YL, Yu CJ, et al. Randomized, placebo-controlled, phase II study of sequential erlotinib and chemotherapy as first-line treatment for advanced non-small-cell lung cancer. J Clin Oncol 2009;27:5080–7.
[4] Soda M, Choi YL, Enomoto M, et al. Identification of the transforming EML4-ALK fusion gene in non-small-cell lung cancer. Nature 2007;448:561–6.
[5] Mano H. Non-solid oncogenes in solid tumors: EML4-ALK fusion genes in lung cancer. Cancer Sci 2008;99:2349–55.
[6] Soda M, Takada S, Takeuchi K, et al. A mouse model for EML4-ALK-positive lung cancer. Proc Natl Acad Sci USA 2008;105:19893–7.
[7] Christensen JG, Zou HY, Arango ME, et al. Cytoreductive antitumor activity of PF-2341066, a novel inhibitor of anaplastic lymphoma kinase and c-Met, in experimental models of anaplastic large-cell lymphoma. Mol Cancer Ther 2007;6:3314–22.
[8] Koivunen JP, Mermel C, Zejnullahu K, et al. EML4-ALK fusion gene and efficacy of an ALK kinase inhibitor in lung cancer. Clin Cancer Res 2008;14: 4275–83.
[9] Kwak EL, Camidge DR, Clark J, et al. Clinical activity observed in a phase I dose escalation trial of an oral c-met and ALK inhibitor, PF-02341066. J Clin Oncol 2009;27:15s.
[10] Bang Y, Kwak EL, Shaw AT, et al. Clinical activity of the oral ALK inhibitor PF-02341066 in ALK-positive patients with non-small cell lung cancer (NSCLC). J Clin Oncol 2010;28:18s [suppl; abstr 3].
[11] Kwak EL, Bang YJ, Camidge DR, et al. Anaplastic lymphoma kinase inhibition in non-small-cell lung cancer. N Engl J Med 2010;363:1693–703.
[12] Takeuchi K, Choi YL, Togashi Y, et al. KIF5B-ALK, a novel fusion oncokinase identified by an immunohistochemistry-based diagnostic system for ALK-positive lung cancer. Clin Cancer Res 2009;15:3143–9.
[13] Inamura K, Takeuchi K, Togashi Y, et al. EML4-ALK lung cancers are characterized by rare other mutations, a TTF-1 cell lineage, an acinar histology, and young onset. Mod Pathol 2009;22:508–15.
[14] Shaw AT, Yeap BY, Mino-Kenudson M, et al. Clinical features and outcome of patients with non-small-cell lung cancer who harbor EML4-ALK. J Clin Oncol 2009;27(September (26)):4247–53.
[15] Takahashi T, Snooze M, Kobayashi M, et al. Clinicopathologic features of non-small-cell lung cancer with EML4-ALK fusion gene. Ann Surg Oncol 2010;17(March (3)):889–97.
[16] Nakajima T, Kimura H, Takeuchi K, et al. Treatment of lung cancer with an ALK inhibitor after EML4-ALK fusion gene detection using endobronchial ultrasound-guided transbronchial needle aspiration. J Thorac Oncol 2010;5:2041–3.
[17] Yasufuku K, Chiyo M, Koh E, et al. Endobronchial ultrasound guided transbronchial needle aspiration for staging of lung cancer. Lung Cancer 2005;50:347–54.
[18] Yasufuku K, Chiyo M, Sekine Y, et al. Real-time endobronchial ultrasound-guided transbronchial needle aspiration of mediastinal and hilar lymph nodes. Chest 2004;126:122–8.
[19] Herth FJ, Eberhardt R, Vilmann P, Krasnik M, Ernst A. Real-time endobronchial ultrasound guided transbronchial needle aspiration for sampling mediastinal lymph nodes. Thorax 2006;61:795–8.
[20] Herth FJ, Ernst A, Eberhardt R, Vilmann P, Dienemann H, Krasnik M. Endobronchial ultrasound-guided transbronchial needle aspiration of lymph nodes in the radiologically normal mediastinum. Eur Respir J 2006;28: 910–4.
[21] Nakajima T, Yasufuku K, Suzuki M, et al. Assessment of epidermal growth factor receptor mutation by endobronchial ultrasound-guided transbronchial needle aspiration. Chest 2007;132:597–602.
[22] Mohamed S, Yasufuku K, Nakajima T, et al. Analysis of cell cycle-related proteins in mediastinal lymph nodes of patients with N2-NSCLC obtained by EBUS-TBNA: relevance to chemotherapy response. Thorax 2008;63:642–7.
[23] Kobayashi S, Boggon TJ, Dayaram T, et al. EGFR mutation and resistance of non-small-cell lung cancer to gefitinib. N Engl J Med 2005;352:786–92.
[24] Lu L, Ghose AK, Quail MR, et al. ALK mutants in the kinase domain exhibit altered kinase activity and differential sensitivity to small molecule ALK inhibitors. Biochemistry 2009;48:3600–9.
[25] Gazdar AF. Activating and resistance mutations of *EGFR* in non-small-cell lung cancer: role in clinical response to EGFR tyrosine kinase inhibitors. Oncogene 2009;28:S24–31.
[26] Choi YL, Soda M, Yamashita Y, et al. EML4-ALK mutations in lung cancer that confer resistance to ALK inhibitors. N Engl J Med 2010;363:1734–9.

Carcinogenesis Advance Access published February 29, 2012

Carcinogenesis vol.0 no.0 pp.1–6, 2012
doi:10.1093/carcin/bgs099
Advance Access publication February 10, 2012

Oncogenic *MAP2K1* mutations in human epithelial tumors

Young Lim Choi[1,2], Manabu Soda[1], Toshihide Ueno[1], Toru Hamada[1], Hidenori Haruta[1], Azusa Yamato[1], Kazutaka Fukumura[2], Mizuo Ando[2], Masahito Kawazu[2], Yoshihiro Yamashita[1] and Hiroyuki Mano[1,2,3,*]

[1]Division of Functional Genomics, Jichi Medical University, Tochigi 329-0498, Japan, [2]Department of Medical Genomics, Graduate School of Medicine, University of Tokyo, Tokyo 113-0033, Japan and [3]Core Research for Evolutional Science and Technology, Japan Science and Technology Agency, Saitama 332-0012, Japan

*To whom correspondence should be addressed. Tel: +81 285 58 7449; Fax: +81 285 44 7322;
Email: hmano@jichi.ac.jp

The scirrhous subtype of gastric cancer is a highly infiltrative tumor with a poor outcome. To identify a transforming gene in this intractable disorder, we constructed a retroviral complementary DNA (cDNA) expression library from a cell line (OCUM-1) of scirrhous gastric cancer. A focus formation assay with the library and mouse 3T3 fibroblasts led to the discovery of a transforming cDNA, encoding for MAP2K1 with a glutamine-to-proline substitution at amino acid position 56. Interestingly, treatment with a MAP2K1-specific inhibitor clearly induced cell death of OCUM-1 but not of other two cells lines of scirrhous gastric cancer that do not carry MAP2K1 mutations, revealing the essential role of MAP2K1(Q56P) in the transformation mechanism of OCUM-1 cells. By using a next-generation sequencer, we further conducted deep sequencing of the *MAP2K1* cDNA among 171 human cancer specimens or cell lines, resulting in the identification of one known (D67N) and four novel (R47Q, R49L, I204T and P306H) mutations within MAP2K1. The latter four changes were further shown to confer transforming potential to MAP2K1. In our experiments, a total of six (3.5%) activating mutations in MAP2K1 were thus identified among 172 of specimens or cell lines for human epithelial tumors. Given the addiction of cancer cells to the elevated MAP2K1 activity for proliferation, human cancers with such MAP2K1 mutations are suitable targets for the treatment with MAP2K1 inhibitors.

Introduction

Many growth-promoting or survival signals converge on members of the RAS family of small guanosine triphosphatases, which then activate the mitogen-activated protein kinase (MAPK) signaling pathway, eventually leading to the transcriptional activation or repression of specific genes in the nucleus (1,2). In addition to such canonical RAS-MAPK signaling, RAS-mediated signaling engages in cross talk with various other signaling pathways, such as those mediated by phosphoinositide 3-kinase (3), Janus kinases (4) as well as WNT and β-catenin (5).

Reflecting the central role of the RAS-MAPK cascade in cell proliferation, activated mutants of RAS family members (HRAS, KRAS and NRAS) are among the oncoproteins most frequently detected in human malignancies (2). Discovery of mutations of BRAF in melanoma and colorectal carcinoma further reinforces the substantial contribution of the RAS-MAPK cascade to carcinogenesis (6). The contributions of somatic mutations of other participants in the RAS-MAPK cascade to human carcinogenesis have remained largely unknown, however.

Gastric cancer is the third most prevalent cancer worldwide and is the second leading cause of cancer-related deaths (>1 million deaths per year) (7). Whereas the diagnosis of gastric cancer has become more sensitive and reliable with the implementation of gastrointestinal endoscopy, unresectable gastric cancer remains mostly intractable. Given the promising efficacy of an inhibitor of the anaplastic lymphoma kinase (ALK) in the treatment of non-small cell lung cancer (NSCLC) positive for the EML4-ALK fusion protein (8,9) and of a BRAF inhibitor in the treatment of melanoma positive for BRAF mutations (10), the identification of additional oncogenes on which cancer cells are dependent should provide a basis for the targeting of such genes in the development of anticancer agents with improved efficacy (11).

We have now adopted the OCUM-1 cell line of scirrhous-type gastric cancer to screen for transforming genes. A retroviral complementary DNA (cDNA) expression library was constructed from the OCUM-1 cells and was then used for a focus formation assay with mouse 3T3 fibroblasts. We thereby identified a transforming mutant of MAP2K1 and further showed that OCUM-1 cells are dependent on MAP2K1 activity for growth. Deep sequencing of *MAP2K1* cDNAs among a total of 171 cancer specimens and cell lines further identified known and novel activating mutations of MAP2K1.

Abbreviations: ALK, anaplastic lymphoma kinase; cDNA, complementary DNA; ERK, extracellular signal-regulated kinase; MAPK, mitogen-activated protein kinase; NSCLC, non-small cell lung cancer.

Materials and methods

Cell lines and specimens

Three cell lines of scirrhous-type gastric cancer (OCUM-1, KATOIII and NUGC-4) were obtained from the Japanese Collection of Research Bioresources (Osaka, Japan), and HEK293 and 3T3 cell lines were obtained from American Type Culture Collection (Manassas, VA). These cells were maintained in Dulbecco's modified Eagle's medium-F12 (Invitrogen, Carlsbad, CA) supplemented with 10% fetal bovine serum and 2 mM L-glutamine (both from Invitrogen). Where indicated, cells were incubated with 20 nM of the MAP2K1 inhibitor AZD6244 (Selleckchem, Houston, TX). Total RNA was extracted from cell lines and cancer specimens with an RNeasy Mini Kit (Qiagen, Valencia, CA) and was subjected to reverse transcription with an oligo(deoxythymidine) primer. Written informed consent was obtained from the subjects who provided cancer specimens, and the study was approved by the human ethics committee of Jichi Medical University.

Focus formation assay

Recombinant ecotropic retroviruses for expression of OCUM-1 cell cDNAs were constructed as described previously (8). Mouse 3T3 cells were infected with the retroviral library at a multiplicity of infection of 0.1 infectious particle per cell, and the cells were then cultured for 2–3 weeks in Dulbecco's modified Eagle's medium-F12 medium supplemented with 5% calf serum (Invitrogen). Genomic DNA was extracted from transformed foci and was subjected to PCR with 5′-PCR primer IIA (Clontech, Mountain View, CA) in order to rescue retrovirus inserts. The nucleotide sequence of rescued cDNAs was determined with a Sanger sequencer.

Functional assay of MAP2K1

The cDNAs for wild-type or mutant forms of MAP2K1 were inserted into the retroviral plasmid pMXS (12), and the modified plasmids were then used to generate recombinant ecotropic retroviruses. Each virus was used to infect 3T3 cells, which were subsequently subjected to a focus formation assay as well as a tumorigenicity assay with nude mice, the latter of which was approved by the institutional review board for animal experiments in Jichi Medical University. The viral plasmids were also used to transfect HEK293 cells by the calcium phosphate method, and the transfected cells were subsequently subjected to immunoblot analysis with antibodies to phosphorylated or total forms of extracellular signal-regulated kinase (ERK) (both from Cell Signaling Technology).

Multiplex deep sequencing of MAP2K1 cDNAs

The entire open reading frame of *MAP2K1* cDNA was amplified by PCR with the primers 5′-AGCGGATCCCCCGGGTCCAAAATGCCC-3′ and 5′-CTTCTCGAGCACTTAGACGCCAGCAGC-3′ from total cDNAs of 171 cancer specimens or cell lines, and the amplification products were fragmented and then subjected to deep sequencing with a Genome Analyzer IIx (GAIIx; Illumina, San Diego, CA) for 76 bases from both ends of each fragment with the paired-end sequencing option. We modified the paired-end adaptors (Illumina) for a multiplex reaction so that an 'N_1N_2' or 'X_2X_1' doublet was added to the 5′or 3′ end, respectively, of cDNA fragments (N_1 and N_2 are any bases

but are complementary to X_1 and X_2, respectively). Fragmented cDNAs of each sample were ligated to our custom paired-end adaptors, and the 'two-base tag' of N_1N_2/X_1X_2 sequences was used to assign read data to the original sample. Given the availability of 16 independent two-base codes, a single lane of the Illumina flow cell can simultaneously run up to 16 samples. The *MAP2K1* mutations identified in the GAIIx data sets were further confirmed by genomic PCR analysis of the corresponding regions of the gene followed by Sanger sequencing.

Results

Identification of MAP2K1(Q56P) in OCUM-1 cells

The scirrhous subtype of gastric carcinoma (diffusely infiltrating carcinoma or Borrmann type IV) is a highly infiltrating poorly differentiated gastric cancer with a 5 year survival rate of only 11.3% (13). Despite the discovery of germ-line mutations in *CDH1* associated with familial diffuse-type gastric cancer (14), such mutations are present at only a relatively low frequency among sporadic cases, and little is known of the driver mutations for this intractable disorder. To identify transforming genes in scirrhous gastric cancer, we constructed a cDNA expression library from a cell line (OCUM-1) established from an individual with this condition. A focus formation assay performed with 3T3 cells infected with the retroviral library resulted in the identification of a dozen transformed foci. Recovery and nucleotide sequencing of insert cDNAs from such foci revealed that one of the cDNAs was derived from human *MAP2K1* with a nucleotide substitution of A-to-C at position 642 of the cDNA (GenBank accession number, NM_002755). Sequencing of this position in OCUM-1 genomic DNA confirmed the presence of this substitution, which results in replacement of a glutamine at amino acid position 56 with proline (Supplementary Figure 1 is available at *Carcinogenesis* Online). MAP2K1, also known as MEK1, functions immediately upstream of MAPK in the MAPK signaling pathway.

Transforming ability of MAP2K1(Q56P)

The MAP2K1(Q56P) mutation was first detected by *in vitro* screening to identify activated components of the RAS-MAPK signaling cascade in rat fibroblasts (15), and it was later identified in a human lung cancer cell line (16). We confirmed the transforming ability of MAP2K1(Q56P) by using a focus formation assay with mouse 3T3 fibroblasts (Figure 1A) and a tumorigenicity assay with nude mice (Figure 1B). Furthermore, such potential of MAP2K1(Q56P) was canceled by eliminating its enzymatic activity (through a replacement of lysine-97 in the adenosine triphosphate-binding pocket to a methionine) or by incubation with a selective MAP2K1/2 inhibitor, AZD6244 (17).

Although the Q56P mutation was previously shown to confer an ~10-fold increase in the enzymatic activity of MAP2K1 (15), little has been known of the dependence of cancer cells on MAP2K1(Q56P) for viability. To address this issue, we compared the effect of AZD6244 on OCUM-1 cells with that on two other cell lines of human scirrhous-type gastric cancer, KATOIII and NUGC-4. Sanger sequencing of genomic DNA from the latter two cell lines confirmed the absence of mutations that could give rise to the Q56P substitution (data not shown). Treatment with AZD6244 inhibited the proliferation of OCUM-1 cells but not that of KATOIII or NUGC-4 cells (Figure 2A), showing that MAP2K1(Q56P) is a suitable target for drug development. Furthermore, in OCUM-1 cells, phosphorylation of ERK1/2 was substantially decreased upon the AZD6244 treatment (Figure 2B) but such effect was less prominent in the other cell lines.

Multiplex deep sequencing of MAP2K1 cDNAs

Given the dependence of OCUM-1 cells on MAP2K1(Q56P) for survival, we next searched for transforming *MAP2K1* mutations in other epithelial tumors. It should be noted, however, that epithelial tumors are frequently contaminated with inflammatory cells and fibrous or necrotic tissue (especially in the case of infiltrative scirrhous-type gastric cancer), which makes it difficult to determine the presence or absence of *MAP2K1* mutations with the use of conventional Sanger sequencing. We therefore chose a deep sequencing approach with the use of a next-generation sequencer. To facilitate simultaneous sequencing of multiple samples, we added two-base tags to the

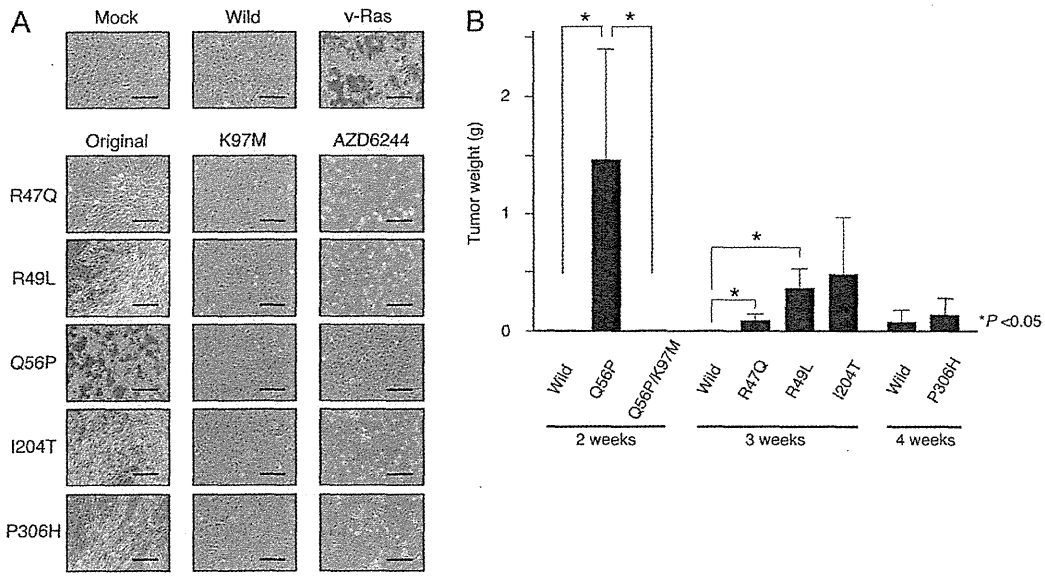

Fig. 1. Transforming potential of MAP2K1 mutants. (**A**) Recombinant retroviruses encoding MAP2K1 (Wild), the indicated MAP2K1 mutants or v-Ras or the corresponding empty virus (Mock), were used to infect 3T3 cells, which were then cultured for 13 days and photographed. Scale bars, 400 μm. The kinase-dead form (K97M) of each mutant was similarly analyzed. In addition to the cells expressing original mutants, the same set of cells was separately treated with 400 nM of AZD6244 for 13 days. (**B**) Mouse 3T3 cells expressing wild-type MAP2K1, Q56P or its kinase-dead form (Q56P/K97M) were injected subcutaneously into the shoulder of nu/nu mice, and tumor weight was examined after 2 weeks. Likewise, tumor weight for the cells expressing wild MAP2K1, R47Q, R49L or I204T mutant was examined after 3 weeks and that for cells expressing wild MAP2K1 or the P306H mutant was examined after 4 weeks. Data are means ± SD of values from four injection sites. The difference in tumor size is evaluated by Student's *t*-test.

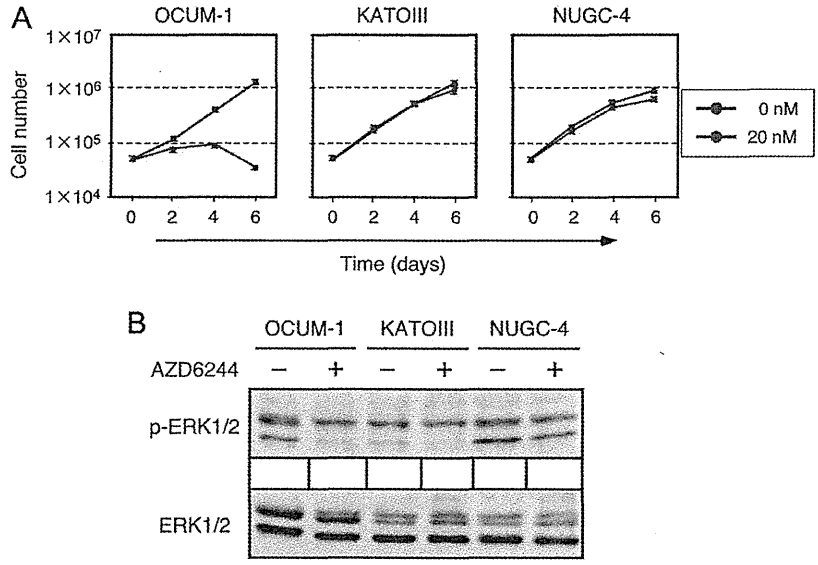

Fig. 2. MAP2K1(Q56P)-dependent growth of OCUM-1 cells. (**A**) OCUM-1, KATOIII and NUGC-4 cells were cultured in the absence or presence of AZD6244 (20 nM), and cell number was determined at the indicated times. Data are means ± SD from three separate experiments. (**B**) Total cell lysates were obtained from each cell line treated with (+) or without (−) 400 nM of AZD6244 for 24 h and probed with antibodies to phosphorylated (p-) or total forms of ERK1/2.

paired-end adaptors used for PCR amplification of fragmented *MAP2K1* cDNAs to be analyzed by a GAIIx sequencer (Figure 3A). The first two bases in each GAIIx read sequence thus correspond to the tag. The diversity of the tag sequences allows a total of 16 independent samples to be analyzed together in a single lane of an Illumina flow cell.

We amplified the entire coding region of *MAP2K1* cDNA from a total of 171 cell lines or clinical specimens of human epithelial cancer, including 26 samples of esophageal cancer (14 cell lines and 12 specimens), 88 samples of gastric cancer (2 cell lines, 46 specimens with a pathological classification of poorly differentiated cell morphology and 40 specimens with well-differentiated cell morphology), 13 samples of breast cancer (2 cell lines and 11 specimens) and 44 specimens of colon cancer. The resulting cDNAs were then subjected to multiplex deep sequencing with four to six different samples (with different tags) run in the same lanes.

A BLAST search of non-synonymous substitutions in the *MAP2K1* sequence revealed an additional five amino acid changes (2.9%) in our 171 samples: I204T in a specimen of poorly differentiated gastric cancer (scirrhous-type), R47Q in a specimen of breast cancer and R49L, D67N and P306H in different specimens of colon cancer (Figure 3B; Supplementary Table 1 is available at *Carcinogenesis* Online). The proportion of mutant reads within the total coverage varied substantially among specimens. For instance, *MAP2K1* reads containing a G-to-A substitution at nucleotide position 140 for the R47Q change in breast cancer occupied ~94% of total reads at this position, suggesting a loss of heterozygosity at the *MAP2K1* locus. In contrast, the reads containing a T-to-C substitution for the I204T change occupied only 7.9% of the total reads from the specimen of scirrhous-type gastric cancer, confirming the low percentage of tumor cells in a given specimen for this highly infiltrative cancer.

We next examined whether these point mutations were somatic alterations by sequencing genomic DNA for the corresponding regions prepared from the tumor as well as paired non-tumor tissue. Unfortunately, an extra specimen for the breast cancer patient (MMK5) was not available, and so we were not able to confirm the genomic change responsible for the R47Q mutation. For this patient, however, the G-to-A change was readily confirmed in cDNA sequencing by the Sanger method (data not shown). For the other four mutations, we did confirm cancer-specific sequence alterations in genomic DNA (Figure 3C). We thus identified a total of six amino acid substitutions in MAP2K1, two (Q56P and D67N) of which had been described previously and had their transforming ability confirmed (16,18), but the remaining four were novel.

Transforming ability of mutant MAP2K1 proteins

To assess the transforming potential of the novel MAP2K1 mutations, we constructed recombinant retroviruses encoding each mutant in order to infect mouse 3T3 fibroblasts. Incubation of the cells for 13 days led to the formation of multiple transformed foci with each mutant but not with wild-type MAP2K1 (Figure 1A). As in the case for the Q56P mutant, no transformed foci were detected for the kinase-dead forms (K97M) or with the incubation with AZD6244. As demonstrated in Figure 1A, a sustained treatment with the compound induced marked cell death among the 3T3 cells except for those expressing the Q56P mutant. Furthermore, it should be noted that the number of transformed foci expressing the R47Q or P306H mutant was substantially fewer than that of cells expressing the other mutants.

Such 3T3 cells were also injected into the shoulder of nu/nu mice (Figure 1B). At 3 weeks after the injection, all of the R47Q, R49L and I204T mutants but not wild-type MAP2K1 or the P306H mutant, generated palpable tumors at every injection site. These data further confirmed the transforming potential of the R47Q, R49L and I204T mutants in addition to Q56P. At 4 weeks after the 3T3 injection, we could identify subcutaneous tumors for the P306H, but the cells expressing wild-type MAP2K1 generated small tumors at several sites as well. Therefore, the transforming potential for MAP2K1(P306H) may be modest.

To examine the effect of the MAP2K1 mutants on the activation status of the downstream kinases ERK1/2, we introduced MAP2K1 or its mutants into HEK293 cells and evaluated the phosphorylation level of ERK1/2 by immunoblot analysis (Figure 3D). Expression of wild-type MAP2K1 resulted in only a small increase in the level of phosphorylation (activation) of ERK1/2. In contrast, MAP2K1(Q56P) induced a marked increase in ERK1/2 activity, whereas a kinase-dead form of this mutant had largely lost this ability, suggesting that MAP2K1(Q56P) activates ERK1/2 in a manner dependent on its enzymatic activity. All of the other mutants tested (R47Q, R49L, I204T and P306H) also markedly increased the level of ERK1/2 phosphorylation, further confirming their activating potential.

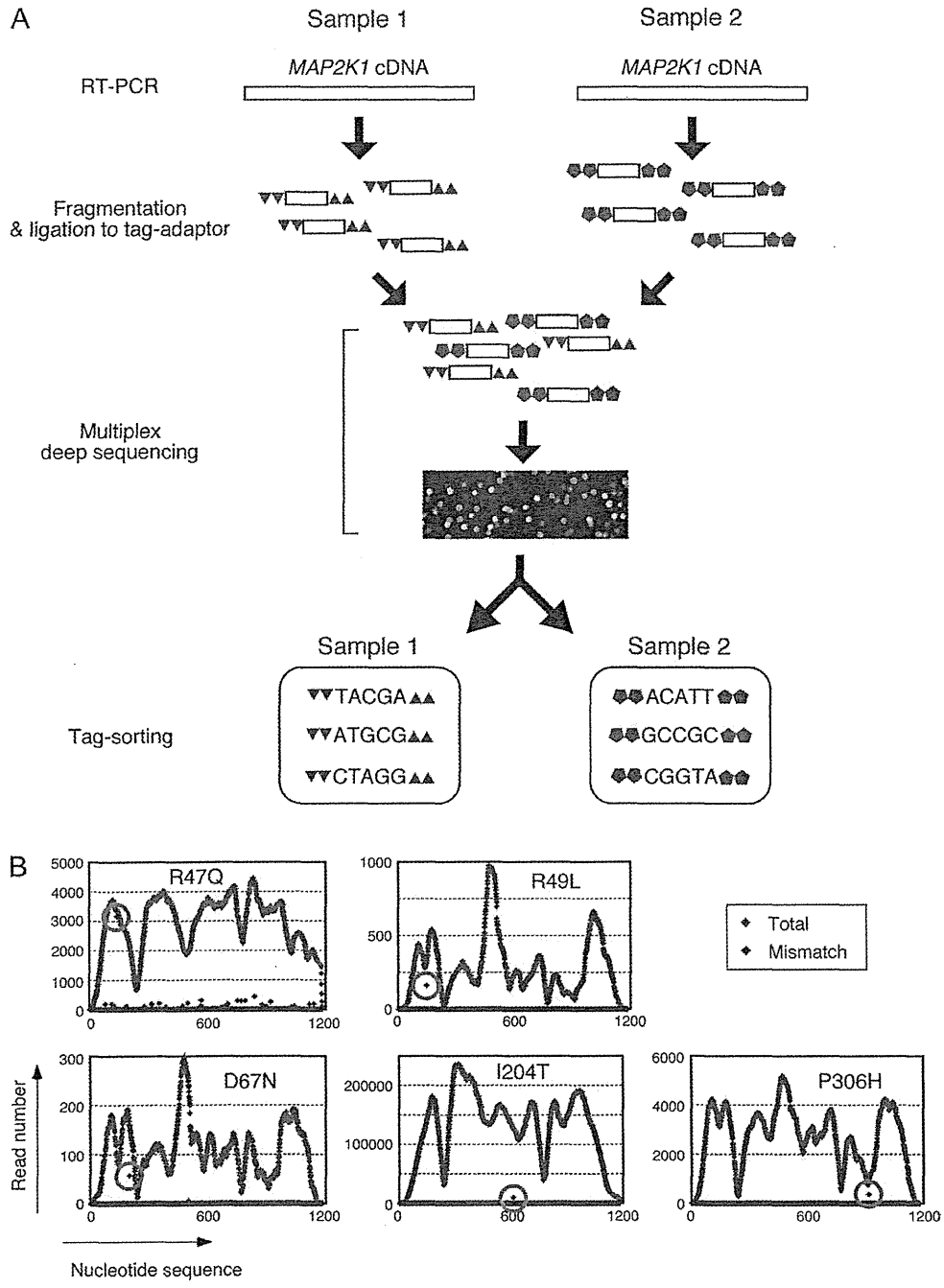

Fig. 3. Multiplex deep sequencing of *MAP2K1* cDNAs. (**A**) *MAP2K1* cDNA was synthesized from 171 cell lines or clinical specimens, fragmented and ligated to sample-specific two-base-tagged adaptors. The cDNA fragments with different two-base tags were mixed and subjected to deep sequencing in the same lane of an Illumina flow cell. The resultant read sequences were sorted, with the two-base tags used as an identification number for each sample. (**B**) *MAP2K1* cDNAs obtained from five cancer specimens harboring the R47Q, R49L, D67N, I204T or P306H mutations were sequenced with the GAIIx system. The numbers for total read coverage (Total) and mismatched reads (Mismatch) are shown at each position of the cDNAs with blue and red diamonds, respectively. The position for mismatched reads for each *MAP2K1* mutation is indicated by a green circle. (**C**) Genomic DNA corresponding to R49, D67, I204 or P306 positions of MAP2K1 was amplified by PCR from tumor and paired normal tissue specimens and was then subjected to Sanger sequencing. Mutated bases are shown in red letters. The PCR product for the tumor harboring the I204T mutation was cloned into a plasmid vector before Sanger sequencing. (**D**) Expression vectors for MAP2K1 (Wild), MAP2K1(Q56P), the kinase-dead mutant MAP2K1(Q56P/K97M), MAP2K1(R47Q), MAP2K1(R49L), MAP2K1(I204T) or MAP2K1(P306H) or the corresponding empty vector (–), were introduced into HEK293 cells. Lysates of the transfected cells were subjected to immunoblot analysis with antibodies to phosphorylated (p-) or total forms of ERK1/2.

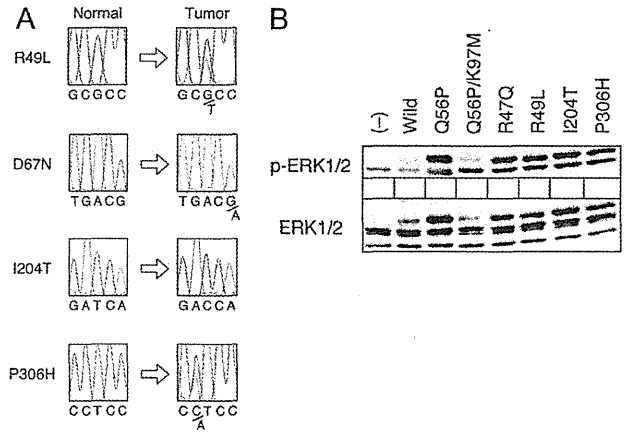

Fig. 3. *continued.*

Discussion

We have identified the Q56P mutant of MAP2K1 in a cell line of scirrhous-type gastric cancer and have shown that these cancer cells are dependent on the mutated MAP2K1 for growth. Furthermore, deep sequencing of *MAP2K1* cDNAs derived from 171 cancer cell lines or clinical specimens revealed one known and four novel mutations of MAP2K1, all of which possess transforming potential. A total of six (3.5%) distinct activating mutations were thus discovered for MAP2K1 in our cohort of 172 cell lines and clinical specimens (Figure 4).

In addition to MAP2K1 mutations identified in individuals with congenital cardiofaciocutaneous syndrome (19), MAP2K1 mutations have been detected in various cancers, albeit infrequently (20). The D67N substitution was discovered in 1 of 15 ovarian cancer cell lines (18). On the other hand, two cases of NSCLC harboring a somatic K57N mutation of MAP2K1 were detected among 207 primary tumor specimens, whereas the Q56P change was identified in 1 of 85 NSCLC cell lines (16). Furthermore, two cases of colorectal cancer harboring a somatic amino acid change (R201H or E203K) of MAP2K1 were detected by screening of 55 cases, but none of 38 cases of breast cancer was found to be associated with a MAP2K1 mutation (21); the same study also found MAP2K1(Y134C) in one cancer cell line. Whereas the Q56P, K57N and D67N substitutions are known to activate MAP2K1, it remains unclear whether these other amino acid changes affect MAP2K1 activity. These previous data, together with our present results, thus suggest that MAP2K1 is infrequently activated by point mutations in various epithelial tumors.

Interestingly, the transforming potential of the MAP2K1 mutants did not correlate always with the phosphorylation level of their downstream targets ERK1/2. While all of R47Q, R49L, Q56P, I204T and P306H mutations similarly induced phosphorylation of ERK1/2 in HEK293 cells (Figure 3D), their transforming potential as judged by 3T3 cells substantially differs (Figure 1). Furthermore, mouse 3T3 cells have a high level of ERK1/2 phosphorylation, and introduction of MAP2K1 mutants only slightly affect the phosphorylation level (data not shown). These data may imply that MAP2K1-dependent transformation of 3T3 cells is, at least, partially mediated through ERK1/2-independent pathways as demonstrated previously (22) or is cell context-dependent.

Known and novel MAP2K1 mutations appear to cluster in two hotspots (Figure 4): a hinge region (R47, R49, Q56, K57 and D67) between the coiled-coil and catalytic domains and the activation loop of the kinase domain (R201, E203 and I204). Amino acid substitutions in the activation loop frequently increase enzymatic activity in a wide variety of protein kinases (23). With regard to the hinge region, artificial truncation of the coiled-coil domain was shown previously to result in constitutive activation of MAP2K1 (24). It is thus likely that

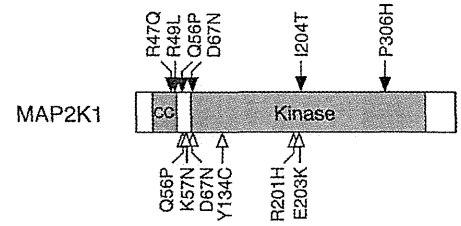

Fig. 4. Schematic representation of the protein structure of MAP2K1 showing amino acid substitutions identified in the present study (closed arrows) and in previous studies (open arrows). CC, coiled-coil domain.

the coiled-coil domain of MAP2K1 negatively regulates enzymatic activity and that mutations that affect the proper structure or function of the coiled-coil domain may release the enzymatic activity of MAP2K1 from such inhibition.

In our study, we took advantage of multiplex deep sequencing to screen for mutations of *MAP2K1* cDNA in a sensitive manner, allowing interrogation of the target cDNA at a high level of coverage among hundreds of samples. Such deep sequencing is likely to be especially important for analysis of specimens of infiltrative tumors or of tumors with large amounts of necrotic tissue, as shown by the detection of the I204T mutation as a low proportion of reads for a specimen of scirrhous-type gastric cancer. Likewise, from pleural effusion of a patient with NSCLC positive for EML4-ALK, we detected a small fraction of tumor cells with acquired mutations responsible for resistance to an ALK inhibitor (25). Such an approach should prove useful for the detection of *MAP2K1* mutations in other types of cancer, and it potentially constitutes a relatively simple, yet highly sensitive, approach to the screening of any target gene or cDNA for nucleotide changes among hundreds of clinical specimens.

Supplementary material

Supplementary Table 1 and Figure 1 can be found at http://carcin.oxfordjournals.org/.

Funding

This study was supported in part by grants for Research on Human Genome Tailor-made and for Third-Term Comprehensive Control Research for Cancer from the Ministry of Health, Labor, and Welfare of Japan, by Grants-in-Aid for Scientific Research (B) and for Young Scientists (A) from the Ministry of Education, Culture, Sports, Science, and Technology of Japan and by grants from the Japan Society

for the Promotion of Science, from Takeda Science Foundation, from the Naito Foundation, from Sankyo Foundation of Life Science, from The Sagawa Foundation for Promotion of Cancer Research, from the Yasuda Medical Foundation, from the Mitsubishi Foundation, and from Kobayashi Foundation for Cancer Research.

Conflict of Interest Statement: None declared.

References

1. Sebolt-Leopold,J.S. *et al.* (2004) Targeting the mitogen-activated protein kinase cascade to treat cancer. *Nat. Rev. Cancer*, **4**, 937–947.
2. Karnoub,A.E. *et al.* (2008) Ras oncogenes: split personalities. *Nat. Rev. Mol. Cell Biol.*, **9**, 517–531.
3. Downward,J. (2008) Targeting RAS and PI3K in lung cancer. *Nat. Med.*, **14**, 1315–1316.
4. Rane,S.G. *et al.* (2000) Janus kinases: components of multiple signaling pathways. *Oncogene*, **19**, 5662–5679.
5. Ishitani,T. *et al.* (1999) The TAK1-NLK-MAPK-related pathway antagonizes signalling between beta-catenin and transcription factor TCF. *Nature*, **399**, 798–802.
6. Davies,H. *et al.* (2002) Mutations of the BRAF gene in human cancer. *Nature*, **417**, 949–954.
7. American Cancer Society. (2008) *Global Cancer Facts and Figures 2007.* http://www.cancer.org/docroot/STT/content/STT_1x_Cancer_Facts_and_Figures_2008.asp?from=fast (22 February 2012, date last accessed).
8. Soda,M. *et al.* (2007) Identification of the transforming *EML4-ALK* fusion gene in non-small-cell lung cancer. *Nature*, **448**, 561–566.
9. Kwak,E.L. *et al.* (2010) Anaplastic lymphoma kinase inhibition in non-small-cell lung cancer. *N. Engl. J. Med.*, **363**, 1693–1703.
10. Flaherty,K.T. *et al.* (2010) Inhibition of mutated, activated BRAF in metastatic melanoma. *N. Engl. J. Med.*, **363**, 809–819.
11. Weinstein,I.B. *et al.* (2006) Mechanisms of disease: oncogene addiction–a rationale for molecular targeting in cancer therapy. *Nat. Clin. Pract. Oncol.*, **3**, 448–457.
12. Onishi,M. *et al.* (1996) Applications of retrovirus-mediated expression cloning. *Exp. Hematol.*, **24**, 324–329.
13. Chen,C.Y. *et al.* (2002) Peritoneal carcinomatosis and lymph node metastasis are prognostic indicators in patients with Borrmann type IV gastric carcinoma. *Hepatogastroenterology*, **49**, 874–877.
14. Guilford,P. *et al.* (1998) E-cadherin germline mutations in familial gastric cancer. *Nature*, **392**, 402–405.
15. Bottorff,D. *et al.* (1995) RAS signalling is abnormal in a c-raf1 MEK1 double mutant. *Mol. Cell. Biol.*, **15**, 5113–5122.
16. Marks,J.L. *et al.* (2008) Novel MEK1 mutation identified by mutational analysis of epidermal growth factor receptor signaling pathway genes in lung adenocarcinoma. *Cancer Res.*, **68**, 5524–5528.
17. Yeh,T.C. *et al.* (2007) Biological characterization of ARRY-142886 (AZD6244), a potent, highly selective mitogen-activated protein kinase kinase 1/2 inhibitor. *Clin. Cancer Res.*, **13**, 1576–1583.
18. Estep,A.L. *et al.* (2007) Mutation analysis of BRAF, MEK1 and MEK2 in 15 ovarian cancer cell lines: implications for therapy. *PLoS ONE*, **2**, e1279.
19. Dentici,M.L. *et al.* (2009) Spectrum of MEK1 and MEK2 gene mutations in cardio-facio-cutaneous syndrome and genotype-phenotype correlations. *Eur. J. Hum. Genet.*, **17**, 733–740.
20. Pao,W. *et al.* (2011) New driver mutations in non-small-cell lung cancer. *Lancet Oncol*, **12**, 175–180.
21. Bentivegna,S. *et al.* (2008) Rapid identification of somatic mutations in colorectal and breast cancer tissues using mismatch repair detection (MRD). *Hum. Mutat.*, **29**, 441–450.
22. Tong,C. *et al.* (2003) Effects of MEK inhibitor U0126 on meiotic progression in mouse oocytes: microtuble organization, asymmetric division and metaphase II arrest. *Cell Res.*, **13**, 375–383.
23. Yamaguchi,H. *et al.* (1996) Structural basis for activation of human lymphocyte kinase Lck upon tyrosine phosphorylation. *Nature*, **384**, 484–489.
24. Mansour,S.J. *et al.* (1994) Transformation of mammalian cells by constitutively active MAP kinase kinase. *Science*, **265**, 966–970.
25. Choi,Y.L. *et al.* (2010) EML4-ALK mutations in lung cancer that confer resistance to ALK inhibitors. *N. Engl. J. Med.*, **363**, 1734–1739.

Received August 5, 2011; revised January 23, 2012;
accepted February 6, 2012

OPEN ACCESS Freely available online

PLoS one

Ex Vivo Expansion of Human CD8$^+$ T Cells Using Autologous CD4$^+$ T Cell Help

Marcus O. Butler[1,2,3], Osamu Imataki[1,2,3], Yoshihiro Yamashita[4], Makito Tanaka[1,2,3], Sascha Ansén[1,2,3], Alla Berezovskaya[1], Genita Metzler[1], Matthew I. Milstein[1], Mary M. Mooney[1], Andrew P. Murray[1], Hiroyuki Mano[4,5], Lee M. Nadler[1,2,3], Naoto Hirano[1,2,3,6,7]*

1 Department of Medical Oncology, Dana-Farber Cancer Institute, Massachusetts, United States of America, **2** Department of Medicine, Brigham and Women's Hospital, Massachusetts, United States of America, **3** Department of Medicine, Harvard Medical School, Boston, Massachusetts, United States of America, **4** Division of Functional Genomics, Jichi Medical University, Tochigi, Japan, **5** Department of Medical Genomics, University of Tokyo, Tokyo, Japan, **6** Immune Therapy Program, Campbell Family Institute for Breast Cancer Research, Campbell Family Cancer Research, Ontario Cancer Institute, Toronto, Ontario, Canada, **7** Department of Immunology, University of Toronto, Toronto, Ontario, Canada

Abstract

Background: Using *in vivo* mouse models, the mechanisms of CD4$^+$ T cell help have been intensively investigated. However, a mechanistic analysis of human CD4$^+$ T cell help is largely lacking. Our goal was to elucidate the mechanisms of human CD4$^+$ T cell help of CD8$^+$ T cell proliferation using a novel *in vitro* model .

Methods/Principal Findings: We developed a genetically engineered novel human cell-based artificial APC, aAPC/mOKT3, which expresses a membranous form of the anti-CD3 monoclonal antibody OKT3 as well as other immune accessory molecules. Without requiring the addition of allogeneic feeder cells, aAPC/mOKT3 enabled the expansion of both peripheral and tumor-infiltrating T cells, regardless of HLA-restriction. Stimulation with aAPC/mOKT3 did not expand Foxp3$^+$ regulatory T cells, and expanded tumor infiltrating lymphocytes predominantly secreted Th1-type cytokines, interferon-γ and IL-2. In this aAPC-based system, the presence of autologous CD4$^+$ T cells was associated with significantly improved CD8$^+$ T cell expansion *in vitro*. The CD4$^+$ T cell derived cytokines IL-2 and IL-21 were necessary but not sufficient for this effect. However, CD4$^+$ T cell help of CD8$^+$ T cell proliferation was partially recapitulated by both adding IL-2/IL-21 and by upregulation of IL-21 receptor on CD8$^+$ T cells.

Conclusions: We have developed an *in vitro* model that advances our understanding of the immunobiology of human CD4$^+$ T cell help of CD8$^+$ T cells. Our data suggests that human CD4$^+$ T cell help can be leveraged to expand CD8$^+$ T cells *in vitro*.

Citation: Butler MO, Imataki O, Yamashita Y, Tanaka M, Ansén S, et al. (2012) Ex Vivo Expansion of Human CD8$^+$ T Cells Using Autologous CD4$^+$ T Cell Help. PLoS ONE 7(1): e30229. doi:10.1371/journal.pone.0030229

Editor: Derya Unutmaz, New York University, United States of America

Received April 7, 2011; **Accepted** December 13, 2011; **Published** January 12, 2012

Funding: This work was supported by the Madeleine Franchi Ovarian Research Fund (MOB), Dunkin Donuts Rising Stars Awards (MOB and NH), a grant from the Cancer Research Institute (LMN), NIH grant K22 CA129240 (NH), NIH grant R01 CA148673 (NH), and the American Society of Hematology Scholar Award (NH). The funders had no role in study design, data collection and analysis, decision to publish, or preparation of the manuscript.

Competing Interests: MOB, LMN and NH have filed a patent application related to aAPC/A2. The patent application number is 10/850,294 and is entitled, "Modified Antigen-Presenting Cells." The authors confirm that this application does not alter their adherence to all PLoS ONE policies on the sharing of data and materials.

* E-mail: nhirano@uhnres.utoronto.ca

Introduction

It is now well accepted that neoplastic cells are immunogenic and that tumors develop in the context of immune recognition by the host [1,2]. Tumor-associated antigens that serve as immune targets include cell lineage differentiation antigens, cancer-testes antigens, and neoantigens produced by mutations in the cancer cell's unstable genome. Mutational events can give rise to multiple immunogenic MHC class I and II restricted, non-self epitopes capable of inducing strong immune responses to the tumor [3,4]. In several malignancies, anti-tumor T cell responses, with infiltration of tumors by CD8$^+$ T lymphocytes and local production of interferon-γ and IL-2, have been associated with improved clinical prognosis [5–8].

Counter regulatory immune responses, however, also develop in the cancer-bearing host. Tumors subvert the immune response by secreting chemotactic factors that recruit immune suppressive elements, thereby inhibiting the function of anti-tumor effectors [9]. Tumor infiltration by T regulatory (Treg) cells has been correlated with inferior clinical outcomes in several tumors [10,11]. These findings have led to the proposal that immune recognition of cancer involves the balancing of opposing forces: anti-tumor effectors vs. pro-tumor regulatory elements [10,12,13]. In fact, a high ratio of Treg cells to CD8$^+$ T cells within the tumor microenvironment has been associated with poorer survival [14,15].

Adoptive T cell therapy is a promising treatment modality designed to amplify the anti-tumor immune response. Anti-tumor effectors are expanded *in vitro*, away from the pro-tumor milieu of the cancer bearing host, and then reinfused as a cellular therapy [16–21]. Successful approaches showing clinical activity include adoptive transfer of tumor antigen-specific T cell lines or clones

that have been derived from the peripheral blood. Specificity can be achieved by stimulating antigen-specific precursor T cells or through genetic modification of expanded bulk T cells to express cloned or chimeric T cell receptor (TCR) genes [22–26]. Alternatively, the nascent, endogenous immune effector response to the tumor can be amplified by expanding tumor-infiltrating lymphocytes (TIL) *in vitro*. Adoptive cell transfer of *in vitro* activated TIL has achieved major clinical responses when patients first undergo lymphodepletion and are then given high dose IL-2 after adoptive transfer [17,27]. Lymphodepletion augments the persistence and function of transferred TIL not only by reducing or temporarily eliminating Treg cells, but also by reducing cytokine sinks that results in the accumulation of homeostatic cytokines such as IL-7 and IL-15 [28,29].

The optimal method for generating clinically effective T cell grafts *in vitro* has yet to be established [21,30]. In order to achieve massive numerical expansion of T cells, current methods necessitate the use of soluble monoclonal antibodies (mAb), allogeneic feeder PBMC, EBV transformed lymphoblastoid cell lines, and/or undefined culture supernatants. Consequently, these requirements present formidable challenges and costs that prevent the widespread clinical application of this therapy. While adoptive transfer of anti-tumor $CD4^+$ T cells can be efficacious, expansion of anti-tumor $CD8^+$ T cells is also an important goal, particularly in light of the association between their persistence and clinical responses [18,31–33].

Insights into requirements for augmenting the expansion of both $CD4^+$ and $CD8^+$ T cells will help further improve methods to generate T cell grafts for adoptive therapy. $CD4^+$ T cells help generate effective immune responses by sustaining $CD8^+$ T cell proliferation, preventing exhaustion, and establishing long-lived functional memory [34]. In mouse models, common γ-chain receptor cytokine and CD40 signaling can mediate $CD4^+$ T cell help [34–44]. In clinical studies, $CD4^+$ T cells have also been implicated in promoting the persistence and anti-tumor activity of antigen-specific $CD8^+$ T cells in patients [45,46]. However, the mechanisms of human $CD4^+$ T cell help are less well understood. To conduct a mechanistic analysis of human $CD4^+$ T cell help, we developed a novel, human cell-based aAPC, aAPC/mOKT3, which induces both $CD4^+$ and $CD8^+$ T cell expansion without allogeneic feeder cells. The removal of allogeneic feeder cells from our T cell culture system enabled us to precisely isolate molecules mediating help of $CD8^+$ T cell expansion that are expressed or secreted by human $CD4^+$ T cells.

Results

K562-based aAPC expressing membranous OKT3 induces $CD3^+$ T cell expansion

We and others have previously reported the generation of aAPC derived from the human erythroleukemia cell line K562 [47–51]. K562 serves as an excellent platform for generating aAPC since it expresses no HLA class I or II molecules, but highly expresses adhesion molecules such as CD54 and CD58. Using K562, we developed a novel aAPC, aAPC/mOKT3, capable of expanding $CD3^+$ T cells regardless of HLA subtype (Figure 1A, Figure S1). This aAPC was engineered to express a membranous form of the anti-CD3 mAb, OKT3, on its cell surface, thus obviating the need for adding soluble mAb to T cell cultures or loading it onto aAPC as described elsewhere [51,52]. aAPC/mOKT3 also ectopically expresses immunostimulatory molecules CD80 and CD83. We and others have shown that CD83 delivers a CD80 dependent signal that promotes lymphocyte longevity [47,53,54].

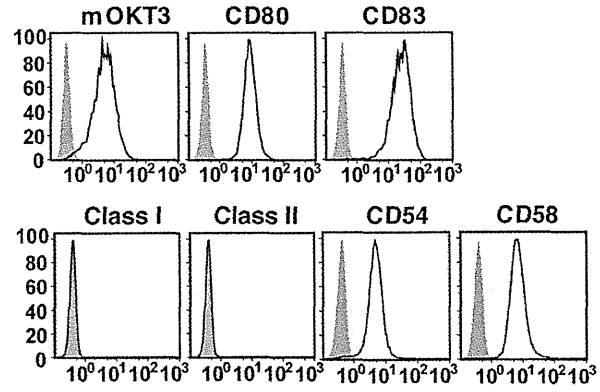

Figure 1. Generation of aAPC/mOKT3. Surface expression of a transduced membranous form of anti-CD3 mAb, and transduced CD80, CD83, and endogenous HLA class I, class II, CD54, and CD58 on aAPC/mOKT3 is shown. A membranous form of anti-CD3 mAb on aAPC/mOKT3 (open) and wild type K562 (shaded) was stained using goat anti-mouse IgG (H+L). Other surface molecules were stained with each specific mAb (open) and isotype control (shaded) and analyzed by flow cytometry. Note the lack of endogenous expression of HLA class I and II on aAPC/mOKT3.
doi:10.1371/journal.pone.0030229.g001

Stimulation of $CD3^+$ T cells with aAPC/mOKT3 induces robust $CD8^+$ T cell expansion

Peripheral $CD3^+$ T cells expanded with aAPC/mOKT3 were phenotypically characterized after 28 days in culture (Figure 2). While the number of both $CD4^+$ and $CD8^+$ T cells increased, $CD8^+$ T cells expanded substantially better than $CD4^+$ T cells, and therefore dominated cultures from every donor tested (Figure 2A). This is in contrast to other pan T cell expansion systems such as anti-CD3/CD28 mAb-coated beads, which invariably favor the expansion $CD4^+$ T cells over $CD8^+$ T cells [55] (Figure 2B). Similar fold expansion of $CD3^+$ T cells was obtained with the aAPC/mOKT3-based and antibody-coated bead-based expansion systems. T cells expanded using aAPC/mOKT3 displayed a central memory~effector memory phenotype ($CD45RA^-$ $CD54RO^+$ $CD62L^{+/-}$) and retained expression of receptors for IL-2, IL-7, and IL-21 (Figure 2C). CD40 ligand was highly expressed by $CD4^+$ T cells but not $CD8^+$ T cells. Importantly, expanded $CD4^+$ $CD25^+$ T cells did not express Foxp3, indicating that immunoinhibitory Treg cells did not proliferate well (Figure 2D).

aAPC/mOKT3 induces unbiased $CD3^+$ T cell expansion, preserving the repertoire for viral and tumor-associated antigens

In order to evaluate whether stimulation with aAPC/mOKT3 induced broad expansion of $CD3^+$ T cells, TCR Vβ repertoire analysis was performed. No obvious skewing in the TCR Vβ usage of both $CD4^+$ and $CD8^+$ T cell populations was revealed, supporting "unbiased" T cell expansion by aAPC/mOKT3 (Figure 3A). Moreover, HLA-restricted antigen-specific $CD8^+$ cytotoxic T lymphocytes (CTL) against viral and tumor antigens could be generated from $CD3^+$ T cells initially expanded for four weeks using aAPC/mOKT3 (Figure 3B and 3C). The functional avidity of these tumor antigen-specific T cells was sufficient to recognize tumor targets endogenously expressing antigen, confirming that the T cell repertoire for tumor antigen recognition was preserved (Figure 3C). We also confirmed that stimulation with aAPC/mOKT3 induced the expansion of tumor-antigen specific T cells. After 28 days in culture, MART1 peptide specific $CD8^+$ T cell expansion was 420–1,150 fold (Figure S1D).

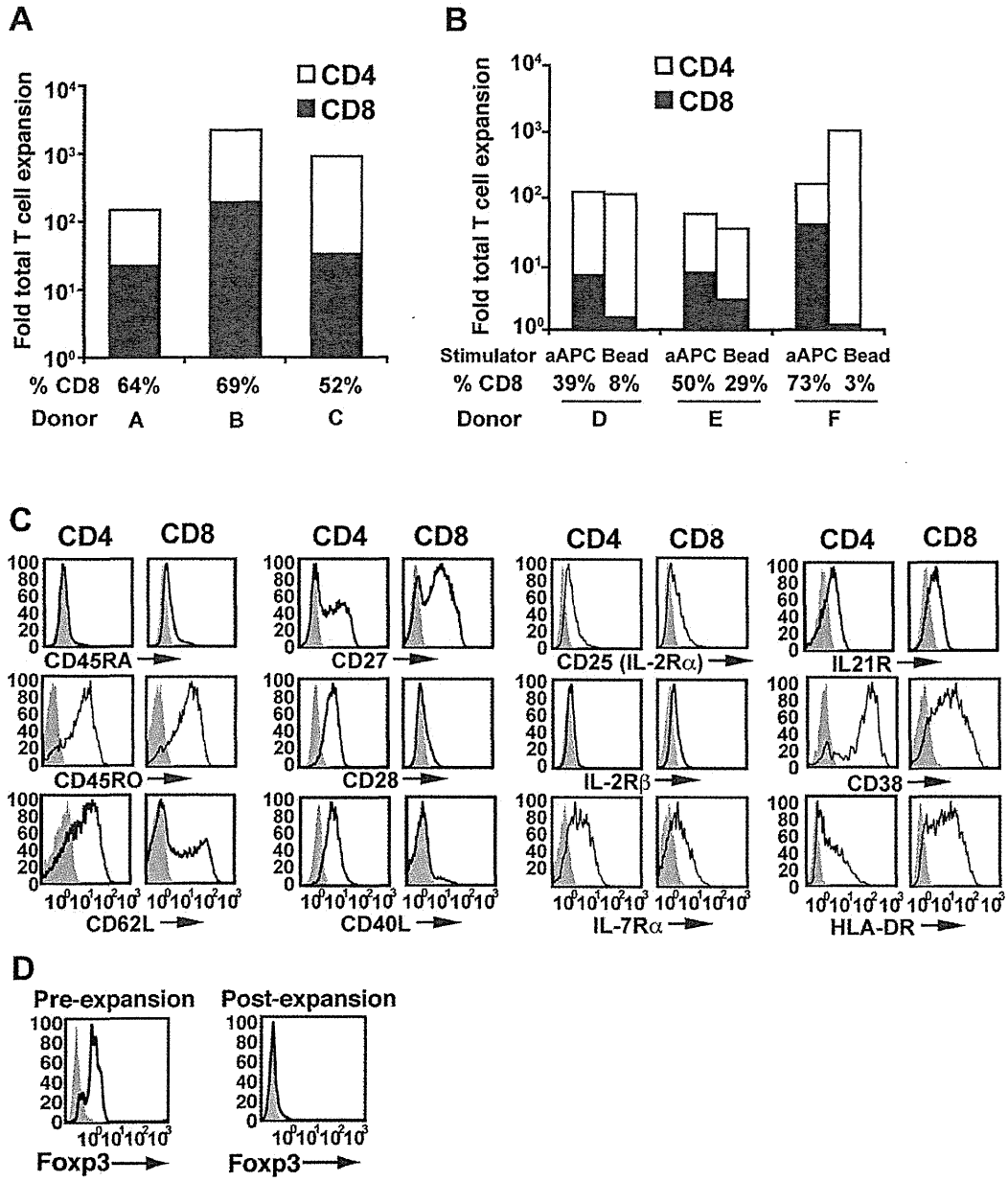

Figure 2. aAPC/mOKT3 expands both CD4+ and CD8+ T cells without using allogeneic feeder PBMC. (**A**) CD3+ T cells were stimulated twice with aAPC/mOKT3 and supplemented with IL-2 between stimulations. Fold expansion of CD3+ T cells over one month is shown for three donors. Shading shows the proportion of expanded CD4+ (white) and CD8+ (black) T cells, and percent CD8+ T cells is indicated. (**B**) CD3+ T cells were stimulated twice with aAPC/mOKT3 or beads (Dynabeads CD3/CD28) and supplemented with IL-2 between stimulations. Fold expansion of CD3+ T cells over one month is shown for three donors. Shading shows the proportion of expanded CD4+ (white) and CD8+ (black) T cells, and percent CD8+ T cells is indicated. (**C**) CD3+ T cells were expanded as described in Figure 2A. Expression of surface molecules on gated CD4+ and CD8+ T cells is shown (open). Isotype mAb staining was used as a control (shaded). (**D**) CD4+ CD25+ Foxp3+ Treg cells, present pre-expansion, were absent in expanded cultures. CD4+ CD25+ cells, pre- and post-expansion, were stained intracellularly with anti-Foxp3 mAb (open) and isotype control (shaded).
doi:10.1371/journal.pone.0030229.g002

aAPC/mOKT3 expands functional TIL but not contaminating Treg cells

Using aAPC/mOKT3, lymphocytes derived from malignant ascites (breast and ovarian cancer) and melanoma metastases were successfully expanded without adding any allogeneic feeder cells (Figure 4A). As observed with peripheral CD3+ T cells in Figure 2A, CD8+ T cells predominantly expanded in all cultures, including those that initially contained a minimal percentage of CD8+ T cells. Importantly, Foxp3+ cells did not proliferate well (Figure 4B). As with peripheral CD3+ T cells, expanded TIL had a central memory~effector memory phenotype (CD45RA- CD62L+/-) consistent with a lack of terminal differentiation (Figure S2). Furthermore, expanded T cells highly expressed CD27 and CD28 which are associated

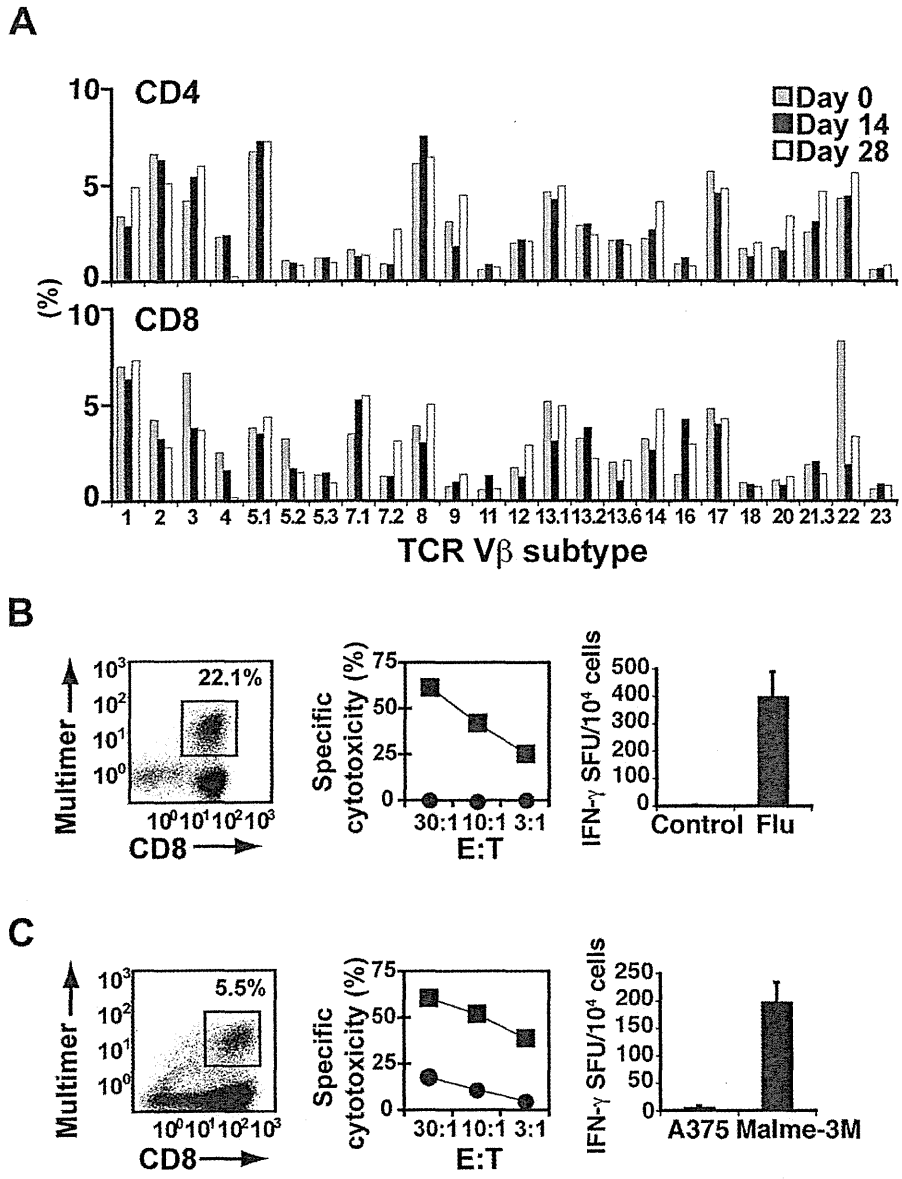

Figure 3. Expansion with aAPC/mOKT3 does not induce skewing of the TCR Vβ repertoire. (**A**) TCR Vβ subfamily analysis before and after stimulation with aAPC/mOKT3 is shown. $CD3^+$ T cells were stimulated with aAPC/mOKT3 on days 0 and 14 and were treated with IL-2 at 300 IU/ml between stimulations. TCR Vβ usage analysis was performed on days 0, 14, 28. Data shown is on gated $CD4^+$ and $CD8^+$ T cells. (**B, C**) $A2^+$ $CD3^+$ T cells were stimulated twice with aAPC/mOKT3 for one month. Subsequently, $CD8^+$ T cells were purified from expanded $CD3^+$ T cells and further stimulated with aAPC/A2 pulsed with Flu or MART1 peptide. (**B**) Flu specificity was demonstrated by multimer staining (left). Functional competence was demonstrated by antigen-specific cytotoxicity (middle) and IFN-γ secretion (right). T2 cells pulsed with Flu peptide (■) or control peptide (●) were used as targets. (**C**) MART1 specificity was similarly demonstrated by multimer staining (left). The HLA-$A2^+$/$MART1^+$ melanoma line, Malme-3M (■), and the HLA-$A2^+$/$MART1^-$ melanoma line, A375 (●), were used as targets in cytotoxicity (middle) and IFN-γ ELISPOT assays (right).
doi:10.1371/journal.pone.0030229.g003

with T cell survival and persistence *in vivo* [56-59]. They also secreted high quantities of IFN-γ and IL-2, while IL-4 secretion was lower and no IL-10 was produced (Figure 4C). These results demonstrate that the aAPC/mOKT3-based system can expand tumor-infiltrating $CD8^+$ T cells in the presence of autologous $CD4^+$ T cells, and that they display phenotypic and functional characteristics consistent with central memory~effector memory T cells.

IL-2 and IL-21 are necessary, but not sufficient, for $CD4^+$ T cell-mediated help of $CD8^+$ T cell expansion

Using the aAPC/mOKT3-based expansion system, we compared the expansion of $CD8^+$ T cells in the presence or absence of $CD4^+$ T cells. $CD8^+$ T cells expanded much better in the presence of $CD4^+$ T cells (Figure 5A), suggesting the presence of $CD4^+$ T cell help for $CD8^+$ T cells in these aAPC/mOKT3-based cultures. We tested whether this "help" was mediated by soluble factors or

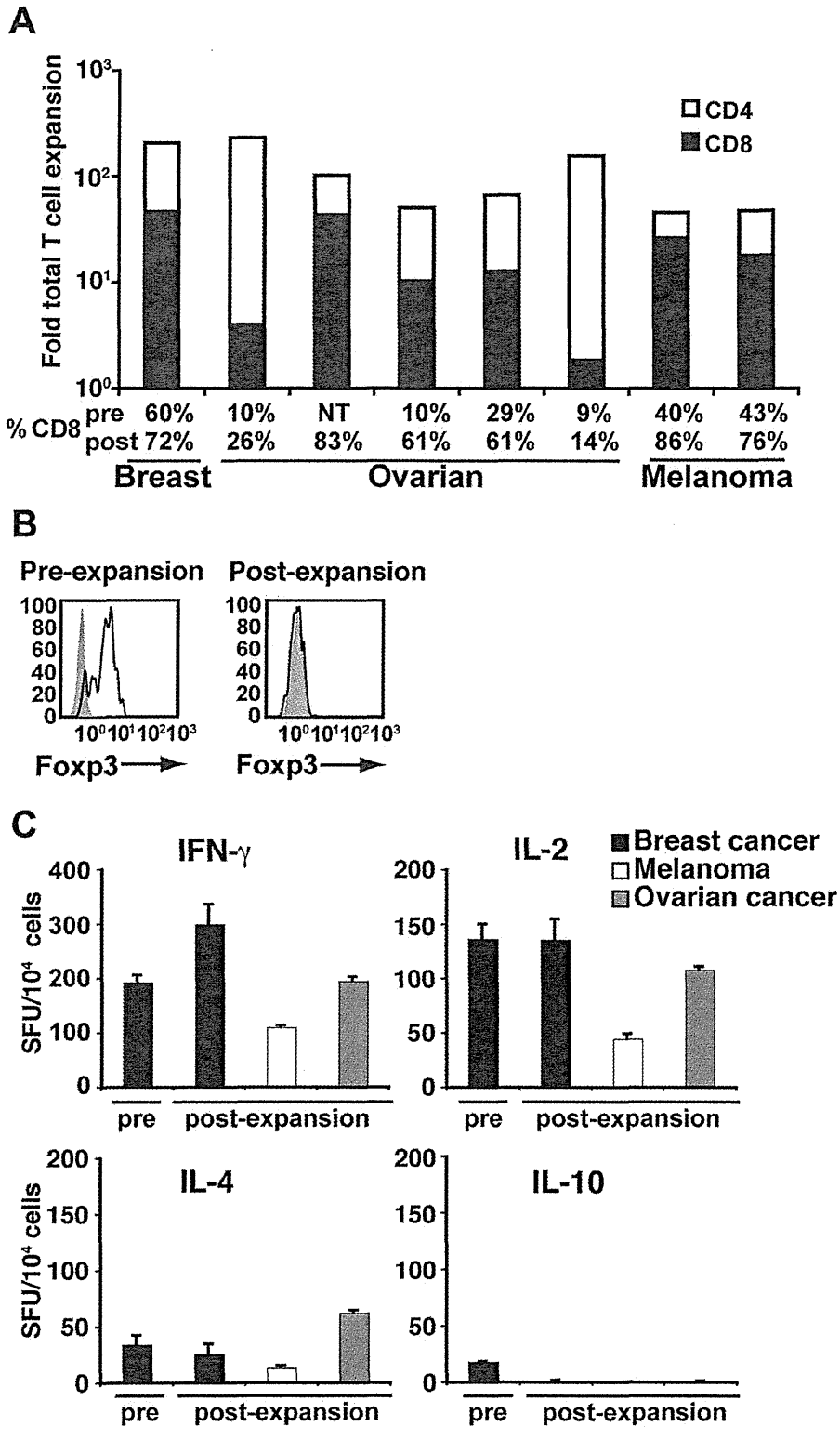

Figure 4. aAPC/mOKT3 expanded TIL are Foxp3 negative and secrete predominantly Th1 cytokines. (**A**) Expansion of TIL obtained from breast and ovarian cancer ascites and melanoma metastases is shown. Shading indicates the proportion of $CD4^+$ (white) and $CD8^+$ (black) T cells in expanded cultures. The percentage of $CD8^+$ T cells in pre- and post-expansion cultures is shown. Note that in all samples tested, the percentage of $CD8^+$ T cells increased even in those that initially contained a minimal percentage of $CD8^+$ T cells. NT denotes not tested. (**B**) $CD4^+$ $CD25^+$ $Foxp3^+$ Treg

cells, present pre-expansion, were not detectable after one month of culture. $CD4^+$ $CD25^+$ cells were intracellularly stained with anti-Foxp3 mAb (open) and isotype control (shaded). (**C**) IFN-γ, IL-2, IL-4, and IL-10 secretion of expanded TIL was determined by ELISPOT assays. Cytokine secretion by TIL from the breast cancer ascites specimen prior to expansion is shown as a control. Pre-expansion samples from melanoma and ovarian cancer specimens were not studied because of low initial cell numbers.
doi:10.1371/journal.pone.0030229.g004

cell-cell contact using the transwell assay (Figure 5B). A single stimulation, without any exogenously added cytokines, expanded $CD8^+$ T cells by an average of 40.5% better when $CD4^+$ T cells were present but separated from $CD8^+$ T cells by the transwell membrane ($P<0.005$). In co-cultures where $CD4^+$ and $CD8^+$ T cells were mixed, allowing for direct cell-cell contact, $CD8^+$ T cells expanded more than in cultures where they were separated from $CD4^+$ T cells by the transwell membrane ($P<0.05$). These results suggest that observed $CD4^+$ T cell help involves both soluble factors and cell-cell contact.

To identify molecules mediating the observed $CD4^+$ T cell help, culture supernatants of $CD4^+/CD8^+$ T cell mixed and separate cultures were tested for a panel of soluble factors (Figure 5C and Table S1). Greater quantities of MIP-1α, MIP-1β, and RANTES were detected in $CD4^+/CD8^+$ T cell mixed cultures compared to separate cultures, suggesting increased production in mixed cultures. In contrast, IL-2 and IL-21, as well as IL-10, IL-17, TNF-α, and TNF-β, were detected at lower levels in mixed cultures, consistent with more consumption or less production of these cytokines.

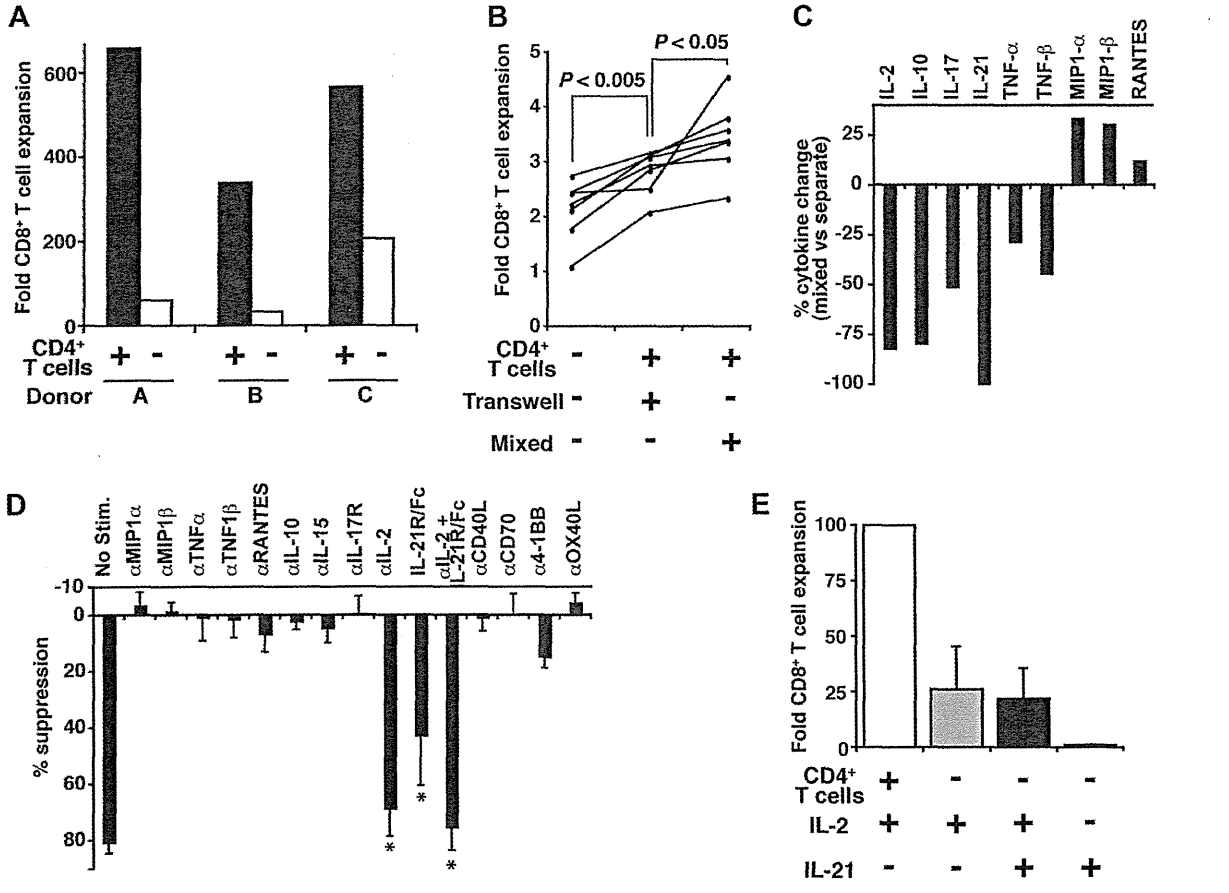

Figure 5. Autologous $CD4^+$ T cell secretion of IL-2/IL-21 is necessary but not sufficient to help $CD8^+$ T cells proliferate. (**A**) $CD8^+$ T cells were stimulated twice by aAPC/mOKT3 with or without $CD4^+$ T cells and treated with IL-2 between stimulations. Fold expansion of $CD8^+$ T cells over 28 days is shown for 3 donors. (**B**) $CD8^+$ T cells were stimulated only once by aAPC/mOKT3 with or without $CD4^+$ T cells in transwell plates. No IL-2 or other cytokines were given. Fold expansion of $CD8^+$ T cells over 6 days is shown for 7 donors. (**C**) Culture supernatants were tested for a panel of soluble factors to identify mediators of $CD4^+$ T cell help. Relative changes in cytokines, comparing mixed vs. separate cultures, are shown. Data is representative of two donors. Absolute values for two donors are shown in Table S1. (**D**) Suppression of $CD8^+$ T cell expansion in the presence of $CD4^+$ T cells by blocking reagents is presented as percent suppression relative to control. Values indicate mean of four independent experiments; error bars show s.d. *$P<0.005$. (**E**) $CD8^+$ T cells were stimulated twice with aAPC/mOKT3 in the presence or absence of $CD4^+$ T cells. IL-2, IL-21, or both were added in each condition. Fold expansion of $CD8^+$ T cells over 28 days is shown. Percent expansion was calculated by dividing the number of expanded $CD8^+$ T cells by the number of $CD8^+$ T cells expanded in the presence of $CD4^+$ T cells. Values indicate mean of six independent experiments; error bars show s.d.
doi:10.1371/journal.pone.0030229.g005

To differentiate between "more consumption" and "less production," $CD4^+/CD8^+$ T cell mixed cultures were stimulated in the presence of blocking reagents, and suppression of $CD8^+$ T cell expansion was assessed (Figure 5D). Blockade of IL-2 and IL-21 resulted in a reduction of expansion by 68.8% ($P<0.005$) and 42.9% ($P<0.005$), respectively. These results indicate that the decreased levels of IL-2 and IL-21 in $CD4^+/CD8^+$ T cell mixed cultures were due to more consumption rather than less production and that these cytokines may be necessary mediators of $CD4^+$ T cell help in this human-based in vitro system. To test whether IL-2/IL-21 could substitute for the observed $CD4^+$ T cell help, $CD8^+$ T cells stimulated with aAPC/mOKT3 were supplemented with IL-2, IL-21, or both (Figure 5E). $CD8^+$ T cells did not expand without IL-2. The addition of IL-2 with or without IL-21 did not improve $CD8^+$ T cell expansion to the level observed when cocultured with $CD4^+$ T cells, demonstrating that IL-2 plus IL-21 are not sufficient to replace $CD4^+$ T cell help.

Exogenous IL-2/IL-21 and upregulation of IL-21 receptor can partially recapitulate $CD4^+$ T cell help of $CD8^+$ T cell expansion *in vitro*

Interestingly, we observed that higher expression of the IL-21 receptor (IL-21R) on $CD8^+$ T cells occurred when $CD4^+$ T cells were present during stimulation by aAPC/mOKT3 (Figure 6A). Higher IL-21R expression on $CD8^+$ T cells was not induced by supplementing cultures with IL-2 and IL-21 (data not shown). This prompted us to hypothesize that increased upregulation of IL-21R on $CD8^+$ T cells is critical for the full effect of IL-21 secreted by $CD4^+$ T cells. We constitutively expressed IL-21R on $CD8^+$ T cells (Figure 6B, left) and stimulated them with aAPC/mOKT3 in the presence of IL-2/IL-21. In accordance with the transduction efficiency of IL-21R to 75.9%, $CD8^+$ T cell proliferation partially increased to levels seen in the presence of $CD4^+$ T cells (Figure 6B, right). This indicates that elevated expression of IL-21R is necessary and can partially recapitulate $CD4^+$ T cell help for $CD8^+$ T cell proliferation.

Discussion

A novel human cell-based aAPC expanded $CD3^+$ T cells *in vitro* without the addition of allogeneic feeder PBMC. Phenotypic analysis of expanded healthy donor T cells and TIL showed, that while both $CD4^+$ and $CD8^+$ T cells expanded, $CD8^+$ T cells predominated. In this model system, we demonstrated that $CD8^+$ T cell expansion depended on the presence of $CD4^+$ T cells, suggesting that $CD4^+$ T cells provided help to proliferating $CD8^+$ T cells. The $CD4^+$ T cell secreted cytokines, IL-2 and IL-21, and the $CD4^+$ T cell-dependent upregulation of IL-21R on $CD8^+$ T cells were necessary for the observed $CD4^+$ T cell help.

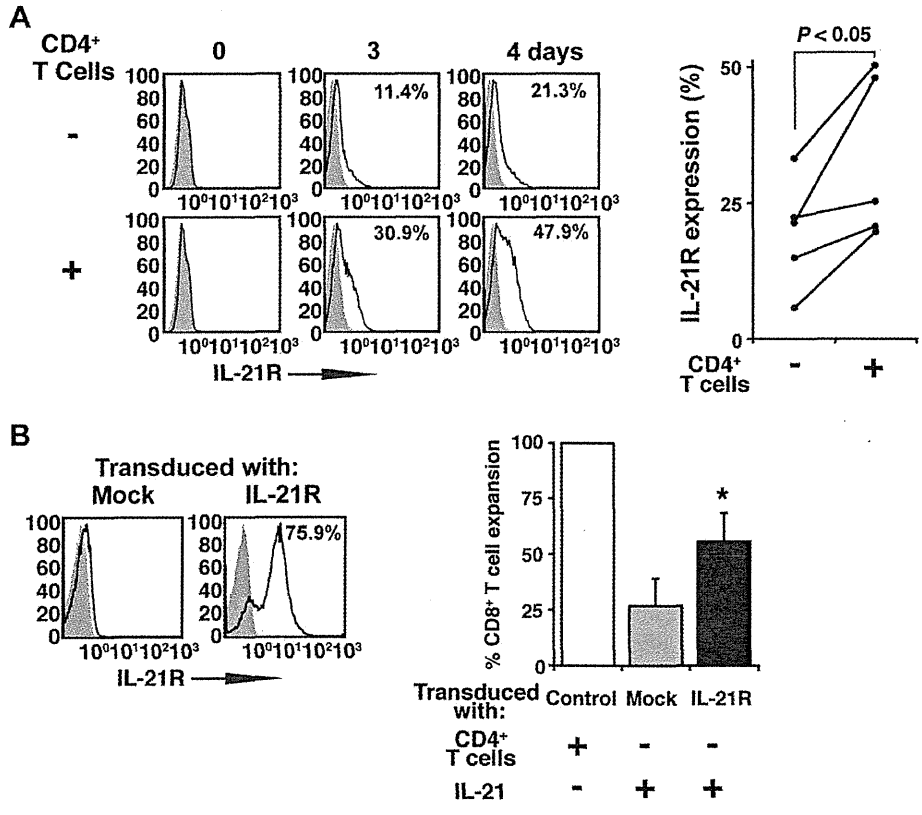

Figure 6. IL-2/IL-21 and upregulation of IL-21R expression replace $CD4^+$ T cell help of $CD8^+$ T cell expansion *in vitro*. (**A**) IL-21R expression on $CD8^+$ T cells stimulated with aAPC/mOKT3 in the presence or absence of $CD4^+$ T cells was studied by flow cytometry. On the left, histogram plots for 1 donor is shown and, on the right, IL-21R expression on day 4 is displayed for 5 donors. (**B**) IL-21R expression on $CD8^+$ T cells ectopically transduced with mock or IL-21R is shown (left). Expansion of transduced $CD8^+$ T cells stimulated twice by aAPC/mOKT3 with or without IL-21 is compared (right). Percent expansion was calculated by dividing the number of expanded transduced $CD8^+$ T cells by that of $CD8^+$ T cells stimulated in the presence of $CD4^+$ T cells. Values indicate mean of four independent experiments; error bars show s.d. *$P<0.005$.
doi:10.1371/journal.pone.0030229.g006

IL-2 and IL-21 have previously been shown to mediate $CD4^+$ T cell help in murine *in vivo* studies. IL-2, one of the few effector cytokines made by naïve $CD4^+$ T cells, expands activated T cells and is essential in the development of $CD8^+$ T cell memory responses to pathogens [60]. While $CD8^+$ T cell responses during acute viral infections were relatively independent of IL-2, the development of protective $CD8^+$ T cell memory responses required IL-2 exposure during priming [35–37]. In vivo models also indicate that IL-21 is critical for containing chronic viral infections and preventing the deletion of high affinity antiviral $CD8^+$ T cells. IL-21 secretion by $CD4^+$ T cells enables the generation, sustained proliferation, and maintenance of polyfunctional $CD8^+$ T cells during chronic infection [39–41].

Our results confirmed a role for IL-2 and IL-21 in human $CD4^+$ T cell help. By using a standardized aAPC, we were able to single out and examine the effects of cocultured $CD4^+$ T cells, unhindered by immunostimulatory and inhibitory factors produced by allogeneic feeder cells. Stimulation of T cells with aAPC/mOKT3 induced the secretion of cytokines and chemokines, including high levels of interferon-γ, MIP-1α, and MIP-1β. Among all the cytokines and chemokines studied, blocking experiments identified IL-2 and IL-21 as necessary for $CD4^+$ T cell help of $CD8^+$ T cell expansion. These cytokines alone, however, were not sufficient to replace $CD4^+$ T cells. We showed that $CD4^+$ T cells help by enhancing IL-21R expression on $CD8^+$ T cells, rendering them more responsive to secreted IL-21. Taken together, the secretion of IL-2/IL-21 and the induction of IL-21R are necessary and sufficient to partially recapitulate human $CD4^+$ T cell help of $CD8^+$ T cell expansion *in vitro*.

Transwell assays showed that the $CD4^+$ T cell dependent expansion of $CD8^+$ T cells was also mediated by cell-cell contact factors. CD40-CD40 ligand interactions have been shown to mediate $CD4^+$ T cell help through CD40-mediated activation of dendritic cells, which are then "licensed" to stimulate $CD8^+$ T cells [43,44,61]. CD40 ligation was also shown to increase IL-21R expression on B lymphocytes suggesting a mechanism for IL-21R upregulation on $CD8^+$ T cells [62]. However, we did not observe any suppression of $CD8^+$ T cell expansion following blockade of CD40 ligand (Figure 5D) even though expanded $CD4^+$ T cells strongly expressed CD40 ligand (Figure 2C). Furthermore, stimulation with aAPC/mOKT3 in the presence of CD40 ligation and the addition of IL-21 did not consistently enhance $CD8^+$ T cell expansion (data not shown). Therefore, these results are in agreement with others who have shown that $CD4^+$ T cells do not provide direct help to $CD8^+$ T cells through CD40 ligation [63,64]. It should be noted that blocking of CD70, 4-1BB, or OX40 signaling also did not suppress the expansion of $CD8^+$ T cells in the presence of $CD4^+$ T cells (Figure 5D).

aAPC induced polyclonal expansion of both $CD4^+$ and $CD8^+$ T cells as shown by the absence of clonal skewing of the TCR Vβ repertoire. The ability to further expand antigen-specific T cells capable of killing tumor targets indicated that the TCR repertoire for highly avid T cells was preserved. Also, expanded TIL secreted higher amounts of Th1 cytokines, IFN-γ and IL-2, which are associated with anti-tumor immunity. While aAPC/mOKT3 induced substantial expansion of $CD8^+$ T cells in the presence of $CD4^+$ T cell help, terminal effector T cell differentiation did not occur, as demonstrated by the central memory~effector memory phenotype ($CD45RA^-$ $CD45RO^+$ $CD62L^{+/-}$). Retention of CD62L expression would enable homing to lymph nodes, where encounter with antigen presented by professional APC could augment immune responses [65]. CD27, which is down-regulated in late stage effector T cells, was also highly expressed. CD27 expression by *in vitro* expanded TIL and T cell clones has been associated with persistence and clinical responses after adoptive transfer [56,57,59,66].

We also found that expanded T cells were not contaminated by cells with the $CD4^+$ $CD25^+$ $Foxp3^+$ Treg phenotype even when $CD4^+$ $CD25^+$ $Foxp3^+$ T cells were present prior to stimulation. We previously found that K562-based aAPC expressing HLA-DR molecules did not expand $Foxp3^+$ cells even though aAPC itself produces modest amounts of the Treg cell growth factor TGF-β [48]. We previously reported that aAPC also secretes IL-6 [47]. It is possible that IL-6, secreted by aAPC, might interfere with $Foxp3^+$ Treg cell expansion [67,68].

Adoptive transfer of *in vitro* expanded T cells has led to clinically significant anti-tumor responses in patients [30]. By leveraging autologous $CD4^+$ T cell help, aAPC/mOKT3 eliminates the use allogeneic feeder cells for T cell expansion, potentially increasing the availability of adoptive therapy as a cancer treatment. We previously reported the development of K562-based aAPCs dedicated to the expansion of HLA-restricted antigen-specific $CD4^+$ and $CD8^+$ T cells [47,48]. Antigen-specific $CD4^+$ and $CD8^+$ T cells expanded *in vitro* with these aAPC had a central memory~effector memory phenotype ($CD45RA^-$ $CD62L^{+/-}$) and possessed surprisingly prolonged *in vitro* longevity without feeder cells or cloning. In a recent clinical trial, HLA-A2-restricted MART1 peptide-specific $CD8^+$ T cells generated *in vitro* with aAPC were infused to advanced melanoma patients [69]. Without lymphodepletion or IL-2 administration, transferred T cells could persist for >16 months, established anti-tumor immunological memory *in vivo*, trafficked to tumor, and induced clinical responses. aAPC/mOKT3 extends the K562 platform to the stimulation of T cells regardless of HLA subtype. The aAPC/mOKT3-based T cell expansion system facilitates the understanding of mechanisms for human $CD4^+$ T cell help and provides a novel strategy to expand T cells for *in vitro* and *in vivo* uses.

Materials and Methods

Ethics Statement

All specimens and clinical data were collected under protocols approved by the Institutional Review Board at the Dana-Farber Cancer Institute (DFCI). All patients provided written informed consent for the collection of samples and subsequent analysis.

cDNAs and cell lines

cDNAs encoding the heavy and light chains for a membranous form of anti-CD3 mAb (OKT3, mIgG2a) were cloned from hybridoma cells (ATCC, VA). HLA null K562 transduced with CD80 and CD83 has been described previously [47,53]. $CD80^+$ $CD83^+$ K562 cells were retrovirally transduced with the heavy and light chains of a membranous form of anti-CD3 mAb. After drug selection, anti-CD3 mAb expressing cells were isolated by magnetic bead guided sorting (Miltenyi Biotec, CA). High expression of a membranous form of anti-CD3 mAb on the cell surface was confirmed by flow cytometry. The parental cell line K562 lacks the endogenous expression of any HLA molecule, but does endogenously express the adhesion molecules CD54 and CD58.

Retrovirus supernatants expressing IL-21R was harvested from PG13 cells. Fresh $CD8^+$ T cells purified from healthy donors were first activated with anti-CD3 (0.75 μg/ml) and anti-CD28 (1 μg/ml) mAbs (Fitzgerald Industries International, MA) for two days. Pre-activated T cells were infected with IL-21R or mock retrovirus supernatants every 24 hr at an MOI of 10 for 10 days and treated with 50 IU/ml IL-2 between infections. Following the assessment

of IL-21R expression by flow cytometry analysis, infected T cells were stimulated with aAPC/mOKT3.

T2, A375, and Malme-3M cell lines were obtained from ATCC as described elsewhere [47].

T cell expansion

Healthy donor PBMC were obtained by leukapheresis performed at the DFCI Kraft Family Blood Donor Center. Cells were isolated by Ficoll-Hypaque density gradient centrifugation and $CD3^+$, $CD4^+$, or $CD8^+$ T cells were purified by negative selection via MACS sorting according to the manufacturer's protocol (Miltenyi Biotec, CA). TIL samples were processed by centrifugation of malignant ascites or mechanical and enzymatic digestion of melanoma metastases with collagenase as previously described [70]. $CD3^+$ TIL were obtained by positive or negative selection via MACS sorting (Miltenyi Biotec, CA). aAPC/mOKT3 cells were irradiated (200 Gy) and added to purified T cells at a T cell to aAPC ratio of 20:1 unless otherwise noted. Dynabeads CD3/CD28 (Invitrogen, CA) were used as stimulators according to the manufacturer's instruction at a T cell to bead ratio of 1:3. Expanding T cells were cultured in RPMI 1640 containing 10% human AB sera and gentamycin (Invitrogen, CA), and between stimulations, unless otherwise noted, 300 IU/ml IL-2 (Prometheus, CA) was added every 3-4 days. In the absence of $CD4^+$ T cells, $CD8^+$ T cells expanded only in the presence of IL-2. Where indicated, 50 ng/ml IL-21 (Peprotech, NJ) was added every 3-4 days. Unless otherwise noted, T cells were restimulated every two weeks. Expanded cells were characterized two weeks after the second stimulation. Cell viability was >90% by trypan blue exclusion.

To test whether antigen-specific cultures can be generated from $CD3^+$ T cells polyclonally expanded with aAPC/mOKT3, $CD3^+$ T cells derived from HLA-A*0201 $(A2)^+$ donors were initially stimulated and expanded with aAPC/mOKT3 for one month. Subsequently, $CD8^+$ T cells were purified and further stimulated with Flu or MART1 peptide-pulsed aAPC/A2 as previously described [47,53].

Analysis of cultured T cells

Flow cytometry analysis was performed using mAbs for the following antigens: CD4, CD8, CD25, CD28, CD56, CD62L, and IL-2Rβ (Coulter, CA); CD40 ligand, CD80, IL-7Rα, OX40, OX40 ligand, and 4-1BB (BD Biosciences, CA); CD27, CD45RA, CD45RO and CD83 (Invitrogen, CA); CCR4 and CCR7 (R&D Systems, MN); ICOS, NKG2D, and PD-1 (eBioscience, CA); CD38, Foxp3, HLA-DR, and 4-1BB ligand (Biolegend, CA); CD40 and CD70 (Ancell, MN); IL-21R (R&D Systems, MN; or BD Biosciences, CA). Goat anti-mouse IgG (H+L) Fab (Jackson ImmunoResearch, PA) was used to detect surface expression of murine Ig. Assessment of TCR Vβ subfamily usage was performed using TCR Vβ mAbs (Beta Mark, Coulter, CA).

To assess the production/consumption of soluble factors in T cell cultures, purified $CD4^+$, $CD8^+$, or a 1:1 mixture of $CD4^+$ and $CD8^+$ T cells were stimulated with irradiated aAPC/mOKT3 for 72 hours and supernatants were measured for: GM-CSF, IFN-γ, IL-2, IL-4, IL-10, IL-12, IL-15, IL-17, MIP-1α, MIP-1β, RANTES, TNF-α, TNF-β, and TRAIL (R&D Systems, MN); IL-7 (Diaclone/Cell Sciences, MA); IL-18 (Medical & Biological Laboratories, Japan); and IFN-α (PBL Biomedical Laboratories, NJ). IL-21 (eBiosciences, CA) was measured at 48-hours. Relative changes in cytokines resulting from mixed cultures of $CD4^+$ and $CD8^+$ T cells vs. separate $CD4^+$ and $CD8^+$ T cell cultures were determined by the following formula: (x-y)/y, where x = cytokine secreted by $CD4^+$ and $CD8^+$ T cell mixed co-cultures and y is the average of cytokine produced in separately stimulated $CD4^+$ and $CD8^+$ T cell cultures.

IFN-γ ELISPOT and standard chromium release assays were performed as described elsewhere [47,53]. IL-2, IL-4 and IL-10 ELISPOT assays were performed according to the manufacturer's protocol (R&D Systems, MN).

Transwell and blocking assays

Transwell assays were performed by placing purified $CD4^+$, $CD8^+$, or a mixture of $CD4^+$ and $CD8^+$ T cells into Millicell-24 plate chambers (Millipore) which were separated by a 0.4 μm filter allowing free movement of soluble factors but not cells. T cells were stimulated once with aAPC/mOKT3 in the absence of exogenous cytokines. Six days later, expansion of $CD8^+$ T cells was determined.

Blocking assays were performed in 96-well round bottomed plates where $CD4^+$ and $CD8^+$ T cells were combined 1:1 and then stimulated with irradiated mOKT3/aAPC in the presence of blocking reagents. Blocking mAbs used recognized IL-2, IL-10, IL-15, IL-17R, MIP-1α, MIP-1β, OX40 ligand, RANTES, TNFα, and TNFβ (R&D Systems, MN); 4-1BB (Neomarkers, CA); CD40 ligand (Biolegend, CA); and CD70 (Ancell, MN). IL-21 was blocked using recombinant human IL-21R subunit/Fc chimeric protein (R&D Systems, MN) as previously described [71]. Six days later, $CD8^+$ T cell expansion was determined.

Statistical analysis

Data analysis was performed using the paired, one-sided Student's t-test where $P<0.05$ was considered to be statistically significant.

Supporting Information

Figure S1 K562-based aAPC/mOKT3, expressing a membranous form of anti-CD3 mAb, stimulates $CD3^+$ T cell expansion. **(A)** $CD3^+$ T cells were stimulated twice with aAPC/mOKT3 and supplemented with IL-2 at the following concentrations: 10 IU/ml (gray), 300 IU/ml (white) and 6,000 IU/ml (black). Fold expansion over 28 days is demonstrated. Without IL-2 addition, T cell expansion over the 28-day culture period was minimal. Data for three separate donors is shown. **(B)** $CD3^+$ T cells were stimulated twice with aAPC/mOKT3 at the indicated aAPC: T cell ratios. Cultures were supplemented with IL-2 (300 IU/ml) between stimulations. Fold expansion of $CD3^+$ T cells over one month is shown for two donors. **(C)** Phenotype of fresh healthy donor $CD3^+$ T cells prior to stimulation is depicted to compare with the T cells shown in Figure 2C which were expanded with aAPC/mOKT3. Expression of surface molecules on gated $CD4^+$ and $CD8^+$ T cells is shown (open). Isotype mAb staining was used as a control (shaded). **(D)** HLA-$A2^+$ healthy donor $CD8^+$ T cells were stimulated with MART1 peptide-pulsed aAPC/A2 as previously described [47,53]. MART1 specific T cells were then stimulated twice with aAPC/mOKT3 in the presence of autologous $CD4^+$ T cells. Fold expansion of MART1 T cells over one month is shown for three donors.
(TIF)

Figure S2 TIL expanded with aAPC/mOKT3 express CD27 and CD28 and have a central memory~effector memory phenotype. $CD3^+$ T cells from malignant ovarian ascites were stimulated twice with aAPC/mOKT3, and cultures were supplemented with IL-2 at 300 IU/ml. **(A)** Fresh, unstimulated TIL and **(B)** aAPC/mOKT3 expanded TIL were stained with indicated mAb (open) and isotype control (shaded).

TIL were analyzed after a one month expansion. Data depicted is on gated $CD4^+$ and $CD8^+$ T cells.
(TIF)

Table S1 Soluble factors in T cell cultures stimulated with aAPC/mOKT3. Concentrations of soluble factors (pg/ml) in supernatants of $CD4^+$ separate, or $CD8^+$ separate, and $CD4^+$ and $CD8^+$ mixed T cell cultures stimulated by aAPC/mOKT3 were measured by ELISA. [a]Percent change was calculated as detailed in Methods. [b]not applicable. Data from two different donors is depicted.
(DOC)

Author Contributions

Conceived and designed the experiments: MOB LMN NH. Performed the experiments: MOB OI MT SA AB GM MIM MMM APM NH. Analyzed the data: MOB LMN NH. Contributed reagents/materials/analysis tools: MOB OI YY MT SA HM LMN NH. Wrote the paper: MOB LMN NH.

References

1. Dunn GP, Old LJ, Schreiber RD (2004) The immunobiology of cancer immunosurveillance and immunoediting. Immunity 21: 137–148.
2. Pellegrini M, Mak TW, Ohashi PS (2010) Fighting cancers from within: augmenting tumor immunity with cytokine therapy. Trends Pharmacol Sci 31: 356–363.
3. Segal NH, Parsons DW, Peggs KS, Velculescu V, Kinzler KW, et al. (2008) Epitope landscape in breast and colorectal cancer. Cancer Res 68: 889–892.
4. Parmiani G, De Filippo A, Novellino L, Castelli C (2007) Unique human tumor antigens: immunobiology and use in clinical trials. J Immunol 178: 1975–1979.
5. Zhang L, Conejo-Garcia JR, Katsaros D, Gimotty PA, Massobrio M, et al. (2003) Intratumoral T cells, recurrence, and survival in epithelial ovarian cancer. N Engl J Med 348: 203–213.
6. Marth C, Fiegl H, Zeimet AG, Muller-Holzner E, Deibl M, et al. (2004) Interferon-gamma expression is an independent prognostic factor in ovarian cancer. Am J Obstet Gynecol 191: 1598–1605.
7. Kusuda T, Shigemasa K, Arihiro K, Fujii T, Nagai N, et al. (2005) Relative expression levels of Th1 and Th2 cytokine mRNA are independent prognostic factors in patients with ovarian cancer. Oncol Rep 13: 1153–1158.
8. Mihm MC, Jr., Clemente CG, Cascinelli N (1996) Tumor infiltrating lymphocytes in lymph node melanoma metastases: a histopathologic prognostic indicator and an expression of local immune response. Lab Invest 74: 43–47.
9. Mantovani A, Romero P, Palucka AK, Marincola FM (2008) Tumour immunity: effector response to tumour and role of the microenvironment. Lancet 371: 771–783.
10. Curiel TJ, Coukos G, Zou L, Alvarez X, Cheng P, et al. (2004) Specific recruitment of regulatory T cells in ovarian carcinoma fosters immune privilege and predicts reduced survival. Nat Med 10: 942–949.
11. Kobayashi N, Hiraoka N, Yamagami W, Ojima H, Kanai Y, et al. (2007) FOXP3+ regulatory T cells affect the development and progression of hepatocarcinogenesis. Clin Cancer Res 13: 902–911.
12. Wilke CM, Wu K, Zhao E, Wang G, Zou W (2010) Prognostic significance of regulatory T cells in tumor. Int J Cancer 127: 748–758.
13. Shimizu J, Yamazaki S, Sakaguchi S (1999) Induction of tumor immunity by removing CD25+CD4+ T cells: a common basis between tumor immunity and autoimmunity. J Immunol 163: 5211–5218.
14. Sato E, Olson SH, Ahn J, Bundy B, Nishikawa H, et al. (2005) Intraepithelial CD8+ tumor-infiltrating lymphocytes and a high CD8+/regulatory T cell ratio are associated with favorable prognosis in ovarian cancer. Proc Natl Acad Sci U S A 102: 18538–18543.
15. Gao Q, Qiu SJ, Fan J, Zhou J, Wang XY, et al. (2007) Intratumoral balance of regulatory and cytotoxic T cells is associated with prognosis of hepatocellular carcinoma after resection. J Clin Oncol 25: 2586–2593.
16. Bollard CM, Gottschalk S, Leen AM, Weiss H, Straathof KC, et al. (2007) Complete responses of relapsed lymphoma following genetic modification of tumor-antigen presenting cells and T-lymphocyte transfer. Blood 110: 2838–2845.
17. Dudley ME, Yang JC, Sherry R, Hughes MS, Royal R, et al. (2008) Adoptive cell therapy for patients with metastatic melanoma: evaluation of intensive myeloablative chemoradiation preparative regimens. J Clin Oncol 26: 5233–5239.
18. Hunder NN, Wallen H, Cao J, Hendricks DW, Reilly JZ, et al. (2008) Treatment of metastatic melanoma with autologous CD4+ T cells against NY-ESO-1. N Engl J Med 358: 2698–2703.
19. Mackensen A, Meidenbauer N, Vogl S, Laumer M, Berger J, et al. (2006) Phase I study of adoptive T-cell therapy using antigen-specific CD8+ T cells for the treatment of patients with metastatic melanoma. J Clin Oncol 24: 5060–5069.
20. Peggs KS, Verfuerth S, Pizzey A, Khan N, Guiver M, et al. (2003) Adoptive cellular therapy for early cytomegalovirus infection after allogeneic stem-cell transplantation with virus-specific T-cell lines. Lancet 362: 1375–1377.
21. Berger C, Turtle CJ, Jensen MC, Riddell SR (2009) Adoptive transfer of virus-specific and tumor-specific T cell immunity. Curr Opin Immunol 21: 224–232.
22. Morgan RA, Dudley ME, Wunderlich JR, Hughes MS, Yang JC, et al. (2006) Cancer regression in patients after transfer of genetically engineered lymphocytes. Science 314: 126–129.
23. Pule MA, Savoldo B, Myers GD, Rossig C, Russell HV, et al. (2008) Virus-specific T cells engineered to coexpress tumor-specific receptors: persistence and antitumor activity in individuals with neuroblastoma. Nat Med 14: 1264–1270.
24. Till BG, Jensen MC, Wang J, Chen EY, Wood BL, et al. (2008) Adoptive immunotherapy for indolent non-Hodgkin lymphoma and mantle cell lymphoma using genetically modified autologous CD20-specific T cells. Blood 112: 2261–2271.
25. Lamers CH, Sleijfer S, Vulto AG, Kruit WH, Kliffen M, et al. (2006) Treatment of metastatic renal cell carcinoma with autologous T-lymphocytes genetically retargeted against carbonic anhydrase IX: first clinical experience. J Clin Oncol 24: e20–22.
26. Kershaw MH, Westwood JA, Parker LL, Wang G, Eshhar Z, et al. (2006) A phase I study on adoptive immunotherapy using gene-modified T cells for ovarian cancer. Clin Cancer Res 12: 6106–6115.
27. Dudley ME, Wunderlich JR, Yang JC, Sherry RM, Topalian SL, et al. (2005) Adoptive cell transfer therapy following non-myeloablative but lymphodepleting chemotherapy for the treatment of patients with refractory metastatic melanoma. J Clin Oncol 23: 2346–2357.
28. Gattinoni L, Finkelstein SE, Klebanoff CA, Antony PA, Palmer DC, et al. (2005) Removal of homeostatic cytokine sinks by lymphodepletion enhances the efficacy of adoptively transferred tumor-specific CD8+ T cells. J Exp Med 202: 907–912.
29. Klebanoff CA, Khong HT, Antony PA, Palmer DC, Restifo NP (2005) Sinks, suppressors and antigen presenters: how lymphodepletion enhances T cell-mediated tumor immunotherapy. Trends Immunol 26: 111–117.
30. Rosenberg SA, Dudley ME (2009) Adoptive cell therapy for the treatment of patients with metastatic melanoma. Curr Opin Immunol 21: 233–240.
31. Zhou J, Dudley ME, Rosenberg SA, Robbins PF (2005) Persistence of multiple tumor-specific T-cell clones is associated with complete tumor regression in a melanoma patient receiving adoptive cell transfer therapy. J Immunother 28: 53–62.
32. Robbins PF, Dudley ME, Wunderlich J, El-Gamil M, Li YF, et al. (2004) Cutting edge: persistence of transferred lymphocyte clonotypes correlates with cancer regression in patients receiving cell transfer therapy. J Immunol 173: 7125–7130.
33. Muranski P, Restifo NP (2009) Adoptive immunotherapy of cancer using CD4(+) T cells. Curr Opin Immunol 21: 200–208.
34. Rochman Y, Spolski R, Leonard WJ (2009) New insights into the regulation of T cells by gamma(c) family cytokines. Nat Rev Immunol 9: 480–490.
35. Wilson EB, Livingstone AM (2008) Cutting edge: CD4+ T cell-derived IL-2 is essential for help-dependent primary CD8+ T cell responses. J Immunol 181: 7445–7448.
36. Bachmann MF, Wolint P, Walton S, Schwarz K, Oxenius A (2007) Differential role of IL-2R signaling for CD8+ T cell responses in acute and chronic viral infections. Eur J Immunol 37: 1502–1512.
37. Williams MA, Tyznik AJ, Bevan MJ (2006) Interleukin-2 signals during priming are required for secondary expansion of CD8+ memory T cells. Nature 441: 890–893.
38. Bevan MJ (2004) Helping the CD8(+) T-cell response. Nat Rev Immunol 4: 595–602.
39. Elsaesser H, Sauer K, Brooks DG (2009) IL-21 is required to control chronic viral infection. Science 324: 1569–1572.
40. Yi JS, Du M, Zajac AJ (2009) A vital role for interleukin-21 in the control of a chronic viral infection. Science 324: 1572–1576.
41. Frohlich A, Kisielow J, Schmitz I, Freigang S, Shamshiev AT, et al. (2009) IL-21R on T cells is critical for sustained functionality and control of chronic viral infection. Science 324: 1576–1580.
42. Oh S, Perera LP, Terabe M, Ni L, Waldmann TA, et al. (2008) IL-15 as a mediator of CD4+ help for CD8+ T cell longevity and avoidance of TRAIL-mediated apoptosis. Proc Natl Acad Sci U S A 105: 5201–5206.
43. Schoenberger SP, Toes RE, van der Voort EI, Offringa R, Melief CJ (1998) T-cell help for cytotoxic T lymphocytes is mediated by CD40-CD40L interactions. Nature 393: 480–483.
44. Bennett SR, Carbone FR, Karamalis F, Flavell RA, Miller JF, et al. (1998) Help for cytotoxic-T-cell responses is mediated by CD40 signalling. Nature 393: 478–480.
45. Walter EA, Greenberg PD, Gilbert MJ, Finch RJ, Watanabe KS, et al. (1995) Reconstitution of cellular immunity against cytomegalovirus in recipients of allogeneic bone marrow by transfer of T-cell clones from the donor. N Engl J Med 333: 1038–1044.
46. Haque T, Wilkie GM, Jones MM, Higgins CD, Urquhart G, et al. (2007) Allogeneic cytotoxic T-cell therapy for EBV-positive posttransplantation lymphoproliferative disease: results of a phase 2 multicenter clinical trial. Blood 110: 1123–1131.

47. Butler MO, Lee JS, Ansen S, Neuberg D, Hodi FS, et al. (2007) Long-lived antitumor CD8+ lymphocytes for adoptive therapy generated using an artificial antigen-presenting cell. Clin Cancer Res 13: 1857–1867.
48. Butler MO, Ansen S, Tanaka M, Imataki O, Berezovskaya A, et al. (2010) A panel of human cell-based artificial APC enables the expansion of long-lived antigen-specific CD4+ T cells restricted by prevalent HLA-DR alleles. Int Immunol 22: 863–873.
49. Numbenjapon T, Serrano LM, Singh H, Kowolik CM, Olivares S, et al. (2006) Characterization of an artificial antigen-presenting cell to propagate cytolytic CD19-specific T cells. Leukemia 20: 1889–1892.
50. Suhoski MM, Golovina TN, Aqui NA, Tai VC, Varela-Rohena A, et al. (2007) Engineering artificial antigen-presenting cells to express a diverse array of co-stimulatory molecules. Mol Ther 15: 981–988.
51. Maus MV, Thomas AK, Leonard DG, Allman D, Addya K, et al. (2002) Ex vivo expansion of polyclonal and antigen-specific cytotoxic T lymphocytes by artificial APCs expressing ligands for the T-cell receptor, CD28 and 4-1BB. Nat Biotechnol 20: 143–148.
52. Dudley ME, Wunderlich JR, Shelton TE, Even J, Rosenberg SA (2003) Generation of tumor-infiltrating lymphocyte cultures for use in adoptive transfer therapy for melanoma patients. J Immunother 26: 332–342.
53. Hirano N, Butler MO, Xia Z, Ansen S, von Bergwelt-Baildon MS, et al. (2006) Engagement of CD83 ligand induces prolonged expansion of CD8+ T cells and preferential enrichment for antigen specificity. Blood 107: 1528–1536.
54. Prazma CM, Yazawa N, Fujimoto Y, Fujimoto M, Tedder TF (2007) CD83 expression is a sensitive marker of activation required for B cell and CD4+ T cell longevity in vivo. J Immunol 179: 4550–4562.
55. Levine BL, Bernstein WB, Connors M, Craighead N, Lindsten T, et al. (1997) Effects of CD28 costimulation on long-term proliferation of CD4+ T cells in the absence of exogenous feeder cells. J Immunol 159: 5921–5930.
56. Powell DJ, Jr., Dudley ME, Robbins PF, Rosenberg SA (2005) Transition of late-stage effector T cells to CD27+ CD28+ tumor-reactive effector memory T cells in humans after adoptive cell transfer therapy. Blood 105: 241–250.
57. Ochsenbein AF, Riddell SR, Brown M, Corey L, Baerlocher GM, et al. (2004) CD27 expression promotes long-term survival of functional effector-memory CD8+ cytotoxic T lymphocytes in HIV-infected patients. J Exp Med 200: 1407–1417.
58. Zhou J, Shen X, Huang J, Hodes RJ, Rosenberg SA, et al. (2005) Telomere length of transferred lymphocytes correlates with in vivo persistence and tumor regression in melanoma patients receiving cell transfer therapy. J Immunol 175: 7046–7052.
59. Huang J, Kerstann KW, Ahmadzadeh M, Li YF, El-Gamil M, et al. (2006) Modulation by IL-2 of CD70 and CD27 expression on CD8+ T cells: importance for the therapeutic effectiveness of cell transfer immunotherapy. J Immunol 176: 7726–7735.
60. Waldmann TA (2006) The biology of interleukin-2 and interleukin-15: implications for cancer therapy and vaccine design. Nat Rev Immunol 6: 595–601.
61. Ridge JP, Di Rosa F, Matzinger P (1998) A conditioned dendritic cell can be a temporal bridge between a CD4+ T-helper and a T-killer cell. Nature 393: 474–478.
62. de Totero D, Meazza R, Zupo S, Cutrona G, Matis S, et al. (2006) Interleukin-21 receptor (IL-21R) is up-regulated by CD40 triggering and mediates proapoptotic signals in chronic lymphocytic leukemia B cells. Blood 107: 3708–3715.
63. Lee BO, Hartson L, Randall TD (2003) CD40-deficient, influenza-specific CD8 memory T cells develop and function normally in a CD40-sufficient environment. J Exp Med 198: 1759–1764.
64. Sun JC, Bevan MJ (2004) Cutting edge: long-lived CD8 memory and protective immunity in the absence of CD40 expression on CD8 T cells. J Immunol 172: 3385–3389.
65. Gattinoni L, Klebanoff CA, Palmer DC, Wrzesinski C, Kerstann K, et al. (2005) Acquisition of full effector function in vitro paradoxically impairs the in vivo antitumor efficacy of adoptively transferred CD8(+) T cells. J Clin Invest 115: 1616–1626.
66. Huang J, Khong HT, Dudley ME, El-Gamil M, Li YF, et al. (2005) Survival, persistence, and progressive differentiation of adoptively transferred tumor-reactive T cells associated with tumor regression. J Immunother 28: 258–267.
67. Korn T, Bettelli E, Oukka M, Kuchroo VK (2009) IL-17 and Th17 Cells. Annu Rev Immunol 27: 485–517.
68. Li MO, Flavell RA (2008) Contextual regulation of inflammation: a duet by transforming growth factor-beta and interleukin-10. Immunity 28: 468–476.
69. Butler M, Friedlander P, Mooney M, Drury L, Metzler M, et al. (2009) Establishing CD8+ T Cell Immunity by Adoptive Transfer of Autologous, IL-15 Expanded, Anti-Tumor CTL with a Central/Effector Memory Phenotype Can Induce Objective Clinical Responses. Blood (ASH Annual Meeting Abstracts) 114: 782-.
70. Soiffer R, Lynch T, Mihm M, Jung K, Rhuda C, et al. (1998) Vaccination with irradiated autologous melanoma cells engineered to secrete human granulocyte-macrophage colony-stimulating factor generates potent antitumor immunity in patients with metastatic melanoma. Proc Natl Acad Sci U S A 95: 13141–13146.
71. Andersson AK, Feldmann M, Brennan FM (2008) Neutralizing IL-21 and IL-15 inhibits pro-inflammatory cytokine production in rheumatoid arthritis. Scand J Immunol 68: 103–111.

JBC Papers in Press. Published on February 7, 2013 as Manuscript M112.415703
The latest version is at http://www.jbc.org/cgi/doi/10.1074/jbc.M112.415703

Mutations in the nucleolar phosphoprotein, nucleophosmin, promote the expression of the oncogenic transcription factor MEF/ELF4 in leukemia cells and potentiates transformation

Koji Ando M.D., Ph.D.,[1] Hideki Tsushima M.D., Ph.D.,[2] Emi Matsuo M.D., Ph.D.,[3] Kensuke Horio M.D.,[4] Shinya Tominaga-Sato M.D., Ph.D.,[5] Daisuke Imanishi M.D., Ph.D.,[1] Yoshitaka Imaizumi M.D., Ph.D.,[2] Masako Iwanaga M.D., Ph.D., M.P.H.,[1] Hidehiro Itonaga M.D.,[1] Shinichiro Yoshida M.D., Ph.D.,[3] Tomoko Hata M.D., Ph.D.,[2] Ryozo Moriuchi M.D.,[6] Hitoshi Kiyoi M.D., Ph.D.,[7] Stephen Nimer M.D.,[8] Hiroyuki Mano M.D., Ph.D.,[9] Tomoki Naoe M.D., Ph.D.,[7] Masao Tomonaga M.D., Ph.D.,[4] Yasushi Miyazaki M.D., Ph.D.[1]

[1]From the Department of Hematology, Atomic Bomb Disease and Hibakusha Medicine Unit, Nagasaki University Graduate School of Biomedical Sciences, Nagasaki, Nagasaki, Japan

[2]Department of Hematology, Nagasaki University Hospital, Nagasaki, Nagasaki, Japan

[3]Department of Hematology, Nagasaki Medical Center, Omura, Nagasaki, Japan

[4]Department of Hematology, Japanese Red-Cross Nagasaki Atomic Bomb Hospital, Nagasaki, Nagasaki, Japan

[5]Division of Hematology, Sasebo City General Hospital, Sasebo, Nagasaki, Japan

[6]Department of Internal Medicine, Keijyu Hospital, Isahaya, Nagasaki, Japan

[7]Department of Hematology and Oncology, Nagoya University Graduate School of Medicine, Nagoya, Japan

[8]Sloan-Kettering Institute, Memorial Sloan-Kettering Cancer Center, New York, NY, USA

[9]Division of Functional Genomics, Jichi Medical University, Shimotsuke, Tochigi, Japan

*Running title: *NPM1 mutations enhance HDM2 expression through MEF/ELF4*

To whom correspondence should be addressed: Yasushi Miyazaki, M.D., Ph.D., Department of Hematology, Atomic Bomb Disease and Hibakusha Medicine Unit, Nagasaki University Graduate School of Biomedical Sciences, 1-12-4 Sakamoto, Nagasaki, Nagasaki 852-8523, Japan, Tel.: +81-95-819-7111; Fax: +81-95-819-7113; E-mail: y-miyaza@nagasaki-u.ac.jp

Keywords: Ets family transcription factor; Leukemia; Oncogene; Promoters; Transcription regulation